N65 10676 N65 10679
(ACCESSION NUMBER) (THRU)
107 1
(PAGES) (CODE)
CR-58971 26
(NASA CR OR TMX OR AD NUMBER) (CATEGORY)
FACILITY FORM 602

MECHANICS OF DEFORMATION AND FRACTURE

Final Report

on

Contract NASw 708

Submitted to: Chief, High Temperature Structures
& Structural Mechanics (Code RV-2)
National Aeronautics & Space Administration
400 Maryland Avenue, S. W.
Washington, D. C. 20025

Prepared by: I. J. Gruntfest & S. J. Becker
General Electric Company
Re-entry Systems Department
P. O. Box 8555
Philadelphia, Pennsylvania 19101

July 1964

MECHANICS OF DEFORMATION AND FRACTURE

Final Report

on

Contract NASw 708

Submitted to: Chief, High Temperature Structures
& Structural Mechanics (Code RV-2)
National Aeronautics & Space Administration
400 Maryland Avenue, S. W.
Washington, D. C. 20025

Prepared by: I. J. Gruntfest & S. J. Becker
General Electric Company
Re-entry Systems Department
P. O. Box 8555
Philadelphia, Pennsylvania 19101

July 1964

THE MECHANICS OF DEFORMATION AND FRACTURE

We are engaged in an exploration of the thermal effects which inevitably accompany the deformation of solids. These effects have been noted often and they are sometimes conspicuous. However, earlier studies have tended to neglect the non-linearities which arise because the deformation processes are likely to be both exothermic and temperature sensitive. Under these conditions regenerative feedback (a chain reaction effect) occurs which enhances the heating and can lead to instability.

Our strategy has been the analysis of the mechanical behavior of highly idealized models of materials with temperature dependent properties. The results of the analyses are then compared with observed phenomena. The idealizations are selected so as to isolate the purely thermal effects in the multifaceted deformation process. Consequently, much that is known about the detailed physics of solids is neglected in the analysis. On the other hand it will be seen that the results are altogether complementary to the modern atomic scale theories and descriptions of the process.

The behavior of the models shows size effects, time effects, rate of loading effects, and rate of strain effects which are similar to those observed experimentally. Furthermore, the introduction of the temperature dependent properties into the continuum theory provides a bridge to the atomic scale theories through the concept of the energy of activation for the atomic scale processes.

The body of this report consists of three separate reports which are being proposed for presentation and publication. The titles and other information about the reports are listed below.

"Apparent Departures from Newtonian Behavior in Liquids Caused by Viscous Heating", Proposed for presentation, 35th Annual Meeting, Society of Rheology, Pittsburgh, Pa., Oct. 1964.

"Thermal Effects in Model Viscoelastic Solids," Proposed for the 6th Annual Structures and Materials Conference, AIAA, Palm Springs, Cal., April, 1965.

"Combined Thermal and Geometric Effects in Viscous ~~Solids~~ Materials," Will be sent to the American Society of Mechanical Engineers.

The reports are attached and separated from one another by colored spacer pages.

N65 10677

APPARENT DEPARTURES FROM NEWTONIAN BEHAVIOR IN LIQUIDS CAUSED BY VISCOUS HEATING

A Report proposed for presentation at the
35th Annual Meeting of
The Society of Rheology
Pittsburgh, Pennsylvania
October 26-28, 1964

Prepared by:

I. J. Gruntfest
RE-ENTRY SYSTEMS DEPARTMENT
GENERAL ELECTRIC COMPANY
P. O. Box 8555
Philadelphia, Pennsylvania
[illegible]

June 1964

ABSTRACT 10677

As part of a general study of the flow and deformation of materials with temperature dependent properties, ideal Couette flow of ~~some~~ incompressible Newtonian liquids is considered here. Equations for the time dependent temperature and velocity distributions in the liquid are solved, numerically, for a variety of stress programs and thermal boundary conditions. The results are compared with closed form analytical solutions that can be obtained in special cases. Instabilities due to regenerative thermal feedback are shown to severely limit the range of shear rates or shear stresses for which steady flows are possible. A new instability mode for the flow with constant average velocity gradient is described which may be connected with the effectiveness of lubricants. Possible relationships of the heating effect to the stability of laminar flows and cavitation in liquids are mentioned. It appears that some apparently non-Newtonian flows can be described more simply when the deviation is attributed to heating than when it is attributed to intrinsic, non-Newtonian behavior. A thermistor circuit analog is demonstrated as an aid to the solution of the Couette flow equations with thermal feedback. author

NOTATION

a – temperature coefficient of the viscosity of the working liquid.

c – the temperature independent, volumetric heat capacity of the working liquid.

E_A – molar energy of activation for the flow process

$\mathcal{G}$ – a convenient non-dimensional group of parameters, or similarity criterion, which defines the initial source strength in the reduced energy equation and is related to the stress.

k – the temperature independent volumetric thermal conductivity of the working liquid.

k_1 – the thermal conductivity of the insulation used to regulate the thermal boundary conditions relative to that of the working liquid.

ℓ – the thickness of the slab of liquid.

t – current real time

T – current local temperature

T_o – an initial or reference temperature.

u – the local velocity in the liquid relative to that at $\xi = o$.

V – the velocity at $\xi = 1$. In terms of the reduced variables it is also the average velocity gradient in the slab.

V_m - the maximum value V can take on for steady flow between isothermal walls.

η - the temperature dependent local viscosity

ξ - the reduced space variable

σ - the current local shear stress

σ_o - the value of σ in the constant stress case, or, the value of σ at $\tau = 1$ in the constant rate of stress increase case, or the initial stress in the constant boundary velocity case.

σ_∞ - the stress at which the temperature becomes unbounded in the adiabatic, constant rate of stress increase case.

τ - the reduced time

τ_∞ - the reduced time at which the temperature becomes unbounded in the adiabatic, constant stress case, or, the reduced time at which the stress decays to one half its initial value in the constant rate of boundary movement case.

τ_∞' - the reduced time at which the temperature becomes unbounded in the adiabatic, constant rate of stress increase case.

ϕ - the reduced temperature

ϕ_c - the reduced temperature on the center plane of the slab of liquid.

ϕ_{cm} - the steady value of ϕ_c which cannot exceed 1.187 in the ideal isothermal wall case.

APPARENT DEPARTURES FROM NEWTONIAN BEHAVIOR IN LIQUIDS CAUSED BY VISCOUS HEATING

INTRODUCTION

The laws of thermodynamics teach that the flow of fluids is never exactly isothermal. On the other hand, rheology, the science of deformation and flow, as defined by Reiner (1), specifically excludes processes which are not isothermal. Orthodox rheologists have made this compromise with reality in order to simplify the mathematical description of the phenomena with which they are concerned. For this they sacrifice completeness in the phenomenological description of flows and lose some contact with the molecular scale details of the processes. Furthermore, some complicated viscosity laws and arbitrary yield conditions must often be invented to compensate for the inadequacies of their model.

Modern developments in mathematical technique and especially   devices for computation have removed some of the incentive for the preservation of mathematical simplicity. It is in this context that a study of the "rheology" of materials with temperature dependent properties has been undertaken. When the model situations are carefully selected, it turns out that the analyses are not formidable, and they provide some new views of the process of flow.

Two earlier reports were concerned with the temperatures generated during ideal viscometric experiments involving Couette (2) and Poisuelle flow (3) at constant stress, and at constant pressure gradient respectively. Criteria were established for significant heating which showed that many experiments of practical and theoretical interest, which have traditionally engaged the attention of rheologists, are far from isothermal. In these cases attention was drawn to time and stress dependencies of the apparent viscosities of Newtonian liquids which are due to the effects of heating.

Once these heating effects are acknowledged, more accurate descriptions of flow processes and improved contact with molecular scale events become possible. Hopefully, some new understanding of the stability of laminar flow and the occurrence of cavitation in liquids will also be developed. The existence of temperature gradients invites convective circulations among streamlines and produces distortions of the velocity profiles, either or both of which could influence the transition to turbulence. The connection with cavitation might be related to the strong dependence of vapor pressures on temperature.

The general question of temperature changes in viscometric experiments has had attention earlier, and many citations are given in references 2 and 3. A recent book on viscometry (4) also reviews earlier work on heating in the flow of liquids. However, the material introduced in references 2 and 3 and elaborated on in this report shows that the book discussion does not take into account the existence of a rather limited range of flow rate and temperature in which steady states of flow are possible. It will be shown here that outside of these ranges an instability mode can appear in liquids, in which the velocity gradient is enhanced in the center of the flow and reduced near the boundaries. This instability provides a mechanism for stress reduction in bearings.

Among the distinctive properties of this instability is the fact that when it occurs, the temperature in the center of the flow increases when the boundaries are cooled! Similar arguments applied to the flow of gases, which become more viscous when heated, would be expected to lead to velocity gradient enhancement at the boundaries and thus might be related to boundary layer formation.

This new type of instability arising in the constant boundary velocity case is related to, but distinguishable from, the thermal instability described in reference 2 which arises in the constant stress case. It is an instability of the latter type which also appears in the constant rate of stress increase case described below.

In this continuing study of thermal effects in deformation and flow, the present report extends the treatment of the Couette flow problem. A range of stress programs and more general thermal boundary conditions are considered. In addition, computed values of the apparent viscosities are presented as well as the local instantaneous values of the central temperatures. While these results have intrinsic practical and theoretical interest, they also serve as a basis for the treatment of more complex models which may include elastic as well as viscous elements and in which geometric changes may accompany the deformations.

DISCUSSION OF ANALYSIS

The strategy of the analysis including viscous heating, and applied to the Couette flow problem, was given in reference 2, and consists of the simultaneous solution of approximate energy and force equations for the instantaneous temperature and velocity distributions in the slab of fluid as functions of the stress history.

The force equation

(1) $$\sigma = \eta \frac{du}{dy}$$

in which σ is the local shearing stress; η is local temperature dependent viscosity and $\frac{du}{dy}$ is the local velocity gradient, requires that the behavior of the liquid be everywhere Newtonian. The temperature dependence of the viscosity for liquids is assumed to be given by

(2) $$\eta = \eta_0 e^{-a(T - T_0)}$$

in which the local viscosity is a function of T, the local temperature and η_0, the viscosity at the reference temperature T_0. The temperature coefficient of viscosity, a, is related to the molar energy of activation for the flow process, E_A, by the approximate relationship

(3) $$a \doteq \frac{E_A}{R T_0^2}$$

in which R is the molar value of Boltzmann's constant.

The approximate energy equation

$$\sigma \frac{du}{dy} = c\,\frac{\partial T}{\partial t} - k\,\frac{\partial^2 T}{\partial y^2} \qquad (4)$$

is composed of three terms. The first is the local instantaneous work rate, or power input, which is the product of the local stress and the local velocity gradient across the slab. The second is the local energy storage rate which is the product of the volumetric heat capacity, c, and the local rate of temperature rise, $\frac{\partial T}{\partial t}$. The third term is the rate of thermal energy loss from the volume element under consideration. It is the product of the thermal conductivity, k, and the second derivative of the temperature with respect to distance across the slab. The instantaneous stress is assumed to be uniform across the slab. This, in effect, neglects accelerations in the fluid. The heat capacity and thermal conductivity of the fluid are assumed to be independent of temperature. This assumption is acceptable for viscous liquids, where the temperature dependence of the viscosity is very much stronger than the temperature dependence of heat capacity and conductivity. For gases, a different viscosity temperature relationship is required, and the Prandtl number, which relates viscosity to thermal conductivity, can be assumed to be constant.

Combining equations 1, 2, and 4 leads to a differential equation relating the local instantaneous temperature to the values of the space and time variables y and t for specified thermal boundary conditions and stress programs.

(5) $$\frac{\sigma^2}{\eta_0} e^{a(T-T_0)} = c\frac{\partial T}{\partial t} - k\frac{\partial^2 T}{\partial y^2}$$

The substitution of the non-dimensional variables

(6) $$\phi = a(T-T_0), \quad \tau = \frac{k}{c\ell^2}t, \quad \xi = \frac{y}{\ell}$$

in which ℓ is the thickness of the slab of fluid leads to the equation

(7) $$\mathcal{Y}\left(\frac{\sigma}{\sigma_0}\right)^2 e^{\phi} = \frac{\partial \phi}{\partial \tau} - \frac{\partial^2 \phi}{\partial \xi^2}$$

in which

(8) $$\mathcal{Y} = \frac{a\,\sigma_0^2\,\ell^2}{k\,\eta_0}$$

The physical significance of the dimensionless quantity or similarity criterion $\mathcal{Y}$ is developed in reference 2.

In general, equation 7 is analytically intractable, and numerical solutions are required. However, special solutions for the adiabatic cases, $\frac{\partial^2 \phi}{\partial \xi^2} = 0$, and for the steady cases, $\frac{\partial \phi}{\partial \tau} = 0$, for particular stress programs and thermal boundary conditions can be obtained in closed form. These are plotted together with the numerical solutions in the figures below.

In all the numerical computations, the thermal boundary conditions are regulated by encasing the slab of working fluid between two slabs of insulation, each having one third the thickness of the working material. The insulating slabs, the outer boundaries of which are held at the initial temperature, have the same volumetric heat capacity as the fluid but their thermal conductivity relative to the fluid is introduced as a parameter k_1. When k_1 is high, the boundaries of the fluid are nearly isothermal. When k_1 is low, the boundaries of the fluid are nearly adiabatic. Many cases appear in which the influence of changes in the thermal boundary conditions on the responses of the fluid overrides the influence of changes in stress.

THE CONSTANT STRESS CASE

The responses of a large slab of liquid subjected to a constant plane shearing stress were discussed in reference 2, and all of the details need not be repeated here. Equation 7 is applicable with $\frac{\sigma}{\sigma_0} = 1$. The essential feature of this case is that as the fluid flows, it becomes hotter. This increases the flow rate, which in turn increases the heating rate. If no heat is removed, the temperature becomes unbounded in the finite time

$$(9) \qquad \tau_\infty = \frac{k\eta_0}{a\sigma_0^2 l^2} = \frac{1}{\mathcal{Y}}$$

If heat is removed at the boundaries of the slab, steady states can develop if the rate of heat generation does not exceed the rate of heat removal. The condition for the existence of steady states depends on the value of the criterion $\mathcal{Y}$ and the thermal boundary conditions described by the parameter k_1.

Numerical solutions for the time dependent central plane temperatures for a range of constant stresses, $\mathcal{Y}$, and thermal boundary conditions are shown in figure 1 in which the time scale is $\mathcal{Y}\tau$ or $\frac{\tau}{\tau_\infty}$.

Figure 2 shows the corresponding time dependent, apparent fluidities (reciprocal viscosities). Notice in both of these figures that curve number 1 lies above curve number 2 even though the stress level is higher for curve 2. This is an example of the effect of thermal boundary conditions overriding the effect of stress. This suggests that viscometers made of different materials, say glass or plastic as compared with metal, could give somewhat different results.

Curves 1 and 2 also exemplify the development of steady states. The magnitude of the steady apparent viscosity, however, is seen to be strongly dependent on the stress and thermal boundary conditions. Effects of this type are often observed in creep experiments (7).

For steady flow at constant stress, equation 7 reduces to

(10) $$\mathcal{Y} e^{\phi} = - \frac{\partial^2 \phi}{\partial \xi^2} ,$$

which has been solved in closed form for the case of isothermal boundaries (9). It is shown that steady flow is not possible when the reduced temperature on the central plane, ϕ_c , exceeds 1.187. This reduced steady temperature is related to the reduced stress $\mathcal{Y}$ in the manner shown in figure 3, derivable from reference 9. The maximum value of $\mathcal{Y}$ is 3.52.

THE CONSTANT RATE OF STRESS INCREASE CASE

If the plane shearing stress increases linearly with time, $\sigma = \sigma_0 \tau$, equation 7 takes the form

$$(11) \qquad y \tau^2 e^{\phi} = \frac{\partial \phi}{\partial \tau} - \frac{\partial^2 \phi}{\partial \xi^2}$$

Here, no steady states are possible because the heating rate constantly increases. If no heat is removed, the energy equation becomes

$$(12) \qquad y \tau^2 e^{\phi} = \frac{d\phi}{d\tau}$$

which can be integrated to give

$$(13) \qquad \frac{y \tau^3}{3} = 1 - e^{-\phi}$$

and it may be seen that the temperature becomes unbounded when

$$(14) \qquad \tau = \tau'_{\infty} = \left(\frac{3}{y}\right)^{1/3}$$

Notice that the adiabatic stress level at this time is given by

$$(15) \qquad \sigma_{\infty} = \sigma_0 \tau'_{\infty} = \left(\frac{3 \sigma_0 k \eta_0}{a l^2}\right)^{1/3}$$

That is, the experiment is terminated by thermal catastrophe at a stress which increases as the cube root of the loading rate. If the onset of thermal instability is viewed as a yield process, this result is in general agreement with many rheological experiments.

The detailed numerical solutions of equation 11 for the reduced temperature on the central plane of the slab of liquid are shown in figure 4. Notice, again, that the effect of thermal boundary conditions can override the effects of stress. Figure 5 shows the inverse of the apparent viscosity as a function of time. The time scale in figure 5, as well as in figure 4 is $y^{1/3}\,\tau$ or τ/τ'_∞. Thermistor analog solutions of equation 11 are discussed in a later section.

THE CONSTANT RATE OF BOUNDARY MOVEMENT CASE

If the average reduced shear rate, V, in the slab of liquid is held constant, the instantaneous value of the stress is defined by the equations

$$(16)\qquad V = \int_0^1 \frac{du}{d\xi}\,d\xi = \frac{\sigma \ell}{\eta_0}\int_0^1 e^{\phi}\,d\xi$$

Equation 7 then takes the form

$$(17)\qquad \mathcal{Y}\frac{e^{\phi}}{\left[\int_0^1 e^{\phi}\,d\xi\right]^2} = \frac{\partial \phi}{\partial \tau} - \frac{\partial^2 \phi}{\partial \xi^2}$$

since

$$\sigma = \frac{\eta_0 V}{\ell \int_0^1 e^{\phi}\,d\xi} = \frac{\sigma_0}{\int_0^1 e^{\phi}\,d\xi}$$

This case is different from the constant stress case because as the process goes on and the liquid becomes hotter, the stress decreases. Thus the rate of heat input decreases.

If no heat is removed, the temperature in the slab is independent of ξ, and the adiabatic energy equation is

$$(18)\qquad \mathcal{Y} e^{-\phi} = \frac{\partial \phi}{\partial \tau}$$

Separating the variables and integrating leads to

$$(19)\qquad \tau = \frac{1}{\mathcal{Y}}\left(e^{\phi} - 1\right) = \tau_\infty\left(e^{\phi} - 1\right)$$

The instantaneous adiabatic stress is then given by

$$(20)\qquad \sigma = \eta_0 V e^{-\phi} = \eta_0 V \frac{1}{1+\frac{\tau}{\tau_\infty}} = \frac{\sigma_0}{1+\frac{\tau}{\tau_\infty}}$$

Here τ_{∞} is not an adiabatic catastrophe time but rather the time required for the stress to decay to one half its initial value. Notice, however, that the adiabatic temperature can increase to any value if the experiment is run long enough. The decay of stress with deformation in this case, which can be very abrupt if the shear rate is high, can be associated with the rheological phenomenon of yield and possibly with fracture.

If heat is removed from the boundaries of the fluid which is subjected to a constant average shear rate, steady states can develop. These steady states, described by solutions of

$$\text{(21)} \qquad y \frac{e^{\phi}}{\left[\int_0^1 e^{\phi} d\xi\right]^2} = -\frac{\partial^2 \phi}{\partial \xi^2} \quad ,$$

must be identical with the steady states developed in the constant stress case and subject to the same limitations of ϕ_c and stress. For the case of ideal isothermal boundaries, these limitations are exhibited in figure 3. This is the rather important point that is not mentioned in reference 4.

To obtain closed form solutions for the steady state, isothermal wall, constant boundary velocity case, we begin with the energy equation (cf equation 4).

$$\frac{a\sigma}{k}\frac{du}{dy} = -\frac{\partial^2 \phi}{\partial y^2} \tag{22}$$

integrating once we obtain

$$\frac{a\sigma}{k}\left(\frac{V}{2} - u\right) = \frac{d\phi}{dy} \tag{23}$$

since $\frac{d\phi}{dy} = 0$ for $u = \frac{V}{2}$.

Now, if 23 is combined with equations 1 and 2 using 6, it becomes

$$\frac{a\eta_0}{k}\left(\frac{V}{2} - u\right)\frac{du}{dy} = e^{\phi}\frac{d\phi}{dy} \tag{24}$$

which can be integrated again to give

$$\frac{a\eta_0}{k}\left(\frac{V}{2}u - \frac{u^2}{2}\right) = e^{\phi} - 1 \tag{25}$$

since $\phi = 0$ when $u = 0$.

If the conditions on the central plane $\phi = \phi_c$ and $u = \frac{V}{2}$ are now substituted into 25, an equation similar to that in reference 4 is obtained.

$$\frac{a\eta_0}{k}\frac{V^2}{8} = e^{\phi_c} - 1. \tag{26}$$

This equation is compatible with those derived for the steady state, isothermal wall, constant stress case except that the range of its applicability is not defined.

When the requirement that $\phi_c \leq 1.187$ generated for the constant stress case is applied, an upper limit on V for steady flow between isothermal walls appears

$$(27) \quad V_m = \left[\frac{(e^{\phi_{cm}} - 1)(8)k}{a\eta_0} \right]^{1/2} = 4.27 \left(\frac{k}{a\eta_0} \right)^{1/2}$$

A typical value of the thermal conductivity of organic liquids is 1.6 X 10^3 (ergs/sec cm^2)(^oC/cm). When the initial viscosity is one poise, a typical value of a is 0.08 $^oC^{-1}$. It follows that the maximum allowable boundary velocity for steady flow would be

$$(28) \quad V_m = 4.27 \left(\frac{1.6 \times 10^3}{(.08)(1)} \right)^{1/2} = 600 \text{ cm/sec}$$

This critical value of V_m decreases as the initial viscosity increases. The point is that measurements made in the middle ranges with many commercial viscometers are outside of the range of steady flow. Notice that below this velocity, temperature effects are not necessarily negligible. For example, close to this value of V_m, the steady, apparent, viscosity differs from η_o by the factor $\int_0^1 e^\phi d\xi = 2.27$.

Returning to the main thread of the discussion, numerical solutions of equation 17 for the temperature on the center plane are presented in figure 6. Notice that curves 5 and 6 for which heat is removed from the boundaries, lie above curve 7 which is for the uncooled case. The reduced apparent viscosities as functions of time are shown in figure 7. Since the apparent viscosities shown by curves 5 and 6 are higher than the adiabatic values, more power is available than in the adiabatic case to support the higher temperatures.

The nature of the instability involved in this case is suggested by the plots of the evolving temperature and velocity profiles (figure 8) in an "experiment" which has no steady state. Notice how the velocity gradient tends to rise in the center and fall near the walls. The latter effect, which is quite dramatic, could account for the low drag on lubricated bearings as well as some of the differences between standing and sliding friction since the drag depends on the wall velocity gradient $\sigma = \eta_0 \left(\frac{du}{dy}\right)_{WALL}$. This also explains how the use of a lubricant with a high viscosity (η_0) can lead to a low drag.

THE THERMISTOR ANALOG

The fact that the resistance of a typical thermistor depends on temperature in the same way as the viscosity of a typical liquid (8) permits the easy construction of an electrical analog for the solution of flow problems with thermal feedback. As an example, the response of a thermistor to the saw tooth voltage program

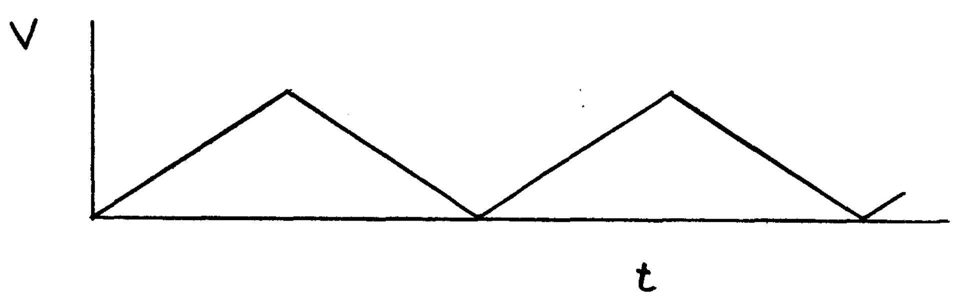

is shown in figure 9.

When the voltage amplitude is low, the current varies linearly with the voltage and, since the heating is negligible, the ascending and descending branches of the current-voltage curve nearly coincide. As the voltage amplitude increases, the temperature rise in the thermistor reduces the resistance and introduces a nonlinearity into the ascending branch. The stored heat changes the shape of the descending branch, opening a hysteresis loop, and causing a drift on cycling. A frequency dependence is also exhibited.

CONCLUDING DISCUSSION

The general relevance of these computations to rheology need not be defended because stress and time dependencies of apparent viscosities are very commonly observed (4). It is important in these cases to separate the "anomolies" due to heating from those due to changes in molecular configurations in the stress field (6). A further point can be made in connection with the "exclusively" Newtonian behavior of low viscosity fluids such as air and water which is often cited (4). In these cases the regime of Newtonian behavior is actually limited by the transition to turbulence. If convective circulations among the streamlines are assumed to be related to the origin of turbulence, and if attention is given to the influence of viscosity on the development of convective circulations (7), the present treatment suggests that, in the case of air and water, the temperature gradients necessary for the onset of convection may be lower than those required for the development of discernible changes in viscosity.

The thermal feedback occurring in ideal Couette flow is the simplest example of a phenomenon which can occur in all real mechanical, electrical and magnetic processes. While the general insights into creep, yield, flow stability, cavitation and lubrication discussed above are likely to be useful, this model can also serve as an element of composite models and can be used to represent other types of processes. For example, application to the breakdown of dielectrics (9), and the limiting strength of solids (10) (11) have been described. Special thermal effects arising in viscoelastic materials subjected to cyclic loading have been discussed by Shapery (12). The wave propagation problem has been considered by Petrof and Gratch (13) and many other questions can be considered.

ACKNOWLEDGEMENTS

The study program which has been discussed in part above has been made possible by the encouragement and support of the Office of Advanced Research and Technology of the National Aeronautics and Space Administration under Contract NASw708 monitored by Messrs. Howard Wolko and Melvin Rosché. The author is also indebted to his colleagues, James Carroll, Paul Gordon, Charles Grebey, George Mueller, and Dr. Stanley Becker for helpful discussions and assistance in performing the analysis and computations.

BIBLIOGRAPHY

1. Reiner, M., Section on Rheology, page 434 et seq., "Encyclopedia of Physics", Volume VI, Edited by S. Flugge, Springer, Berlin (1958).
2. Gruntfest, I. J., "Thermal Feedback in Liquid Flow", Trans. Soc. Rheology, VII, (195-207), 1963.
3. Gruntfest, I. J., J. P. Young and N. L. Johnson, "Temperatures Generated by the Flow of Liquid in Pipes", Jour. Applied Phys., 35 (18-22) 1964.
4. Van Wazer, J. R., J. W. Lyons, K. Y. Kim and R. E. Colwell, "Viscosity and Flow Measurement", Interscience, New York 1963.
5. Reiner, M., "Deformation, Strain and Flow", H. K. Lewis, London 1960, page 217 et seq.
6. Rayleigh, Lord, "On Convection Currents in a Horizontal Layer of Fluid when the Higher Temperature is on the Under Side", Phil. Mag. Series 6, Vol. 32 (Reprinted in Book "Theory of Thermal Convection", B. Salzman, Dover, New York 1962.
7. Nadai, A., "The Theory of Flow and Fracture of Solids", McGraw-Hill, New York, 1950 (page 416).
8. Shive, J. N., "The Properties, Physics and Design of Semi Conductor Devices , D. Van Nostrand, Princeton 1959, page 17.

9. Copple, C., D. R. Hartree, A. Porter and H. Tyson, "The Evaluation of Transient Temperature Distributions in a Dielectric in an Alternating Field", Inst. Elec. Engrs, 85, 56-66 (1939).

10. Gruntfest, I. J., "A Note on Thermal Feedback and the Fracture of Solids", Chapter in Book "Fracture of Solids", Edited by D. C. Drucker and J. J. Gilman, Interscience, New York 1963 (pages 189-193).

11. Gruntfest, I. J., "Thermal Considerations Limiting the Strength of Solids", AIAA Paper #2925-63, presented at Palm Springs, California, April, 1963.

12. Schapery, R. A., "Effect of Cyclic Loading of the Temperature in Viscoelastic Media with Variable Properties", AIAA Journal, 2, 827-835, (May, 1964).

13. Petrof, R. C., and S. Gratch, "Wave Propagation in a Visco Elastic Material with Temperature Dependent Properties and Thermomechanical Coupling", Paper #64-APM-8, Presented to ASME, June 1964, Boulder, Colorado.

CAPTIONS FOR FIGURES

1. The reduced, time-dependent, central plane temperatures, for various values of the reduced constant stress, y , and various thermal boundary conditions k_1.
2. The reduced, time-dependent, apparent fluidity for various values of the reduced constant stress y and various thermal boundary conditions k_1.
3. The steady state reduced central plane temperatures for the isothermal wall case as a function of the reduced constant stress y .
4. The reduced, time-dependent, central plane temperature for various constant rates of stress increase and a function of the rate, σ_0 , and the thermal boundary conditions.
5. The reduced, time-dependent apparent fluidity for various constant rates of stress increase and various thermal boundary conditions.
6. The reduced, time-dependent central plane temperatures for various values of the reduced constant boundary velocity, y, and various thermal boundary conditions.
7. The reduced, time dependent apparent viscosity for various values of the reduced constant boundary velocity, y , and various thermal boundary conditions.

8. The evolving reduced temperature profile (a) and velocity profile (b) for a constant deflection rate case having no steady state.
9. The behavior of the thermistor analog circuit for a saw tooth voltage waveform for different amplitudes and different frequencies.

CONSTANT STRESS

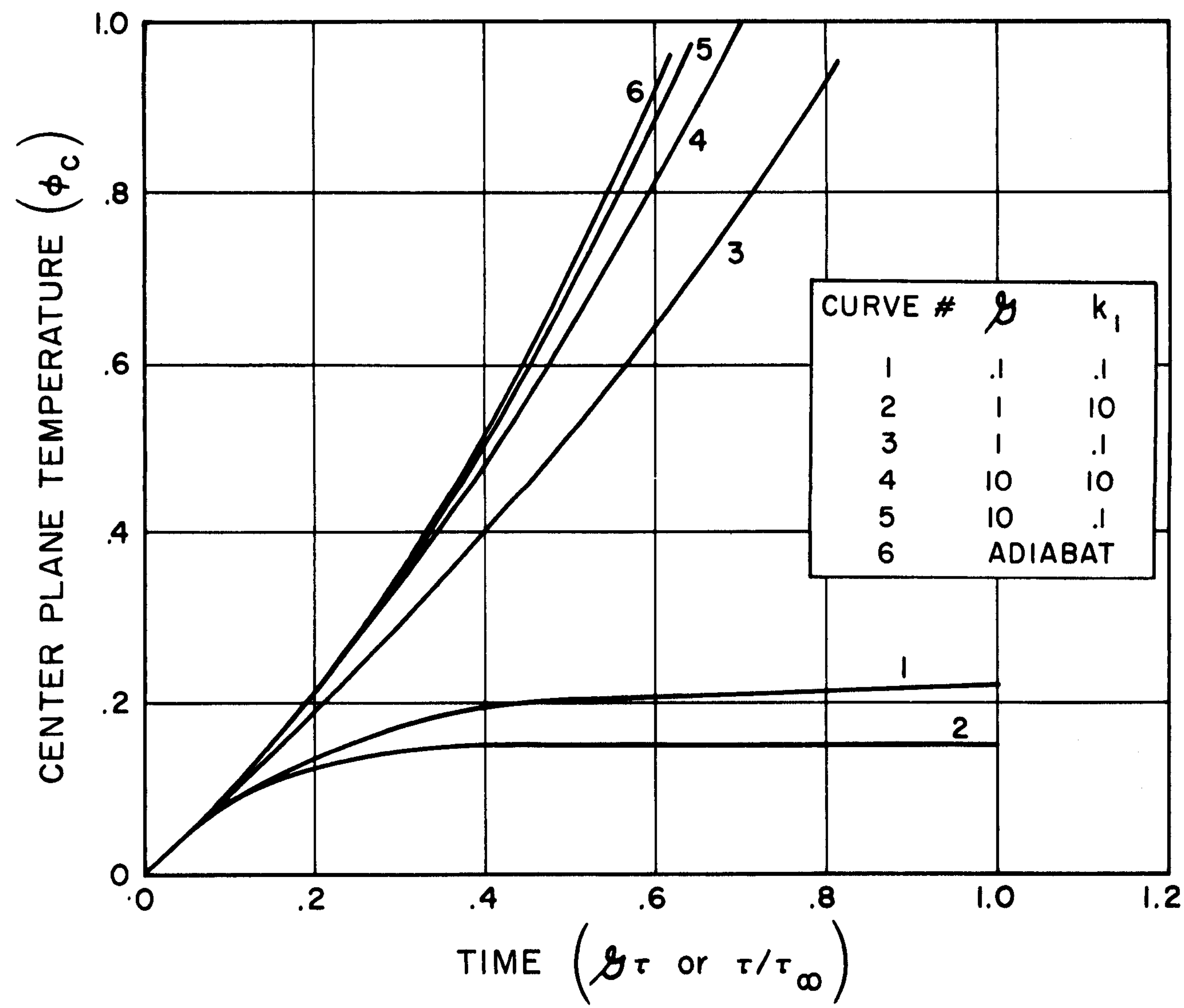

FIG. 1

CONSTANT STRESS

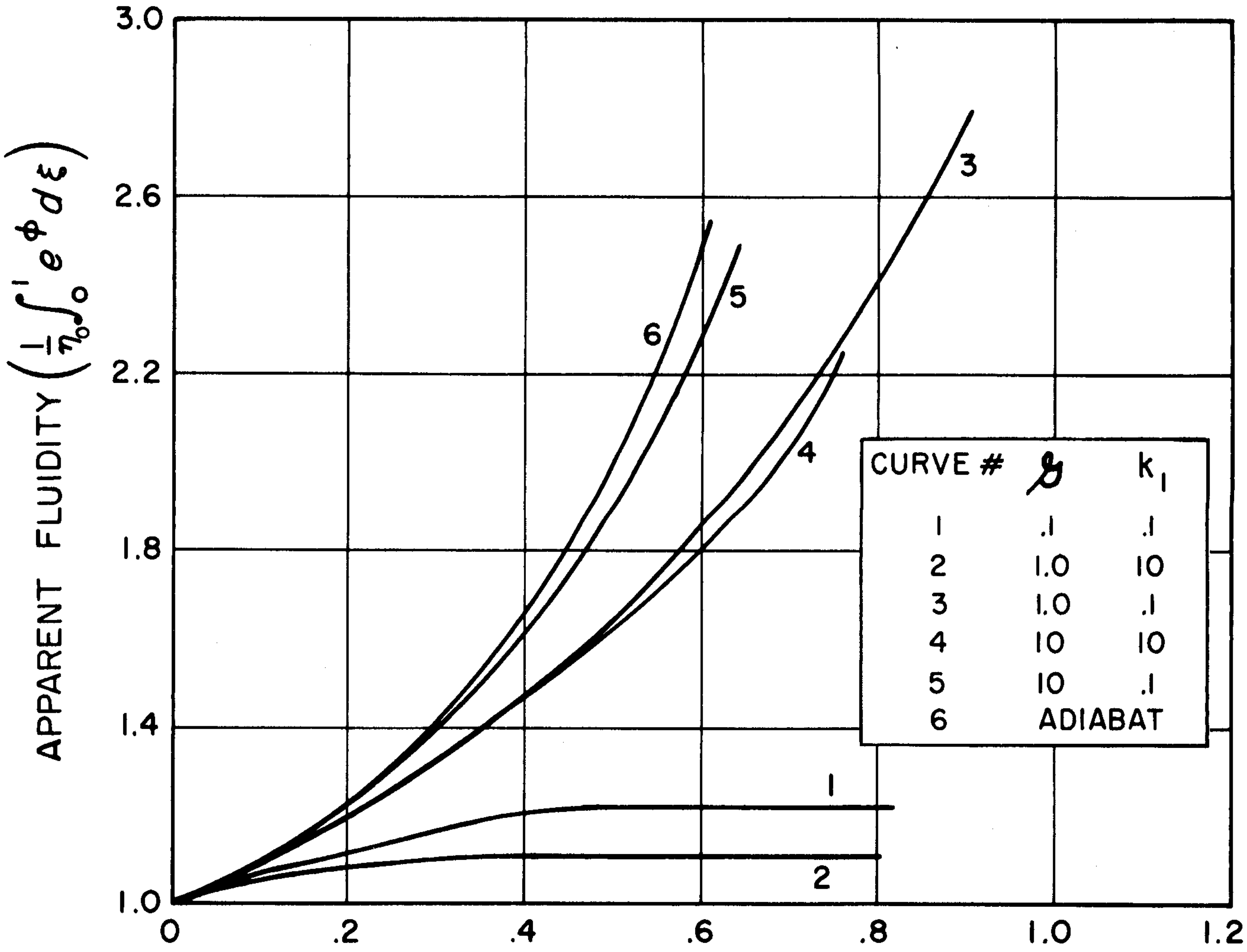

TIME $(\mathcal{G}\tau$ or $\tau/\tau_\infty)$

FIG. 2

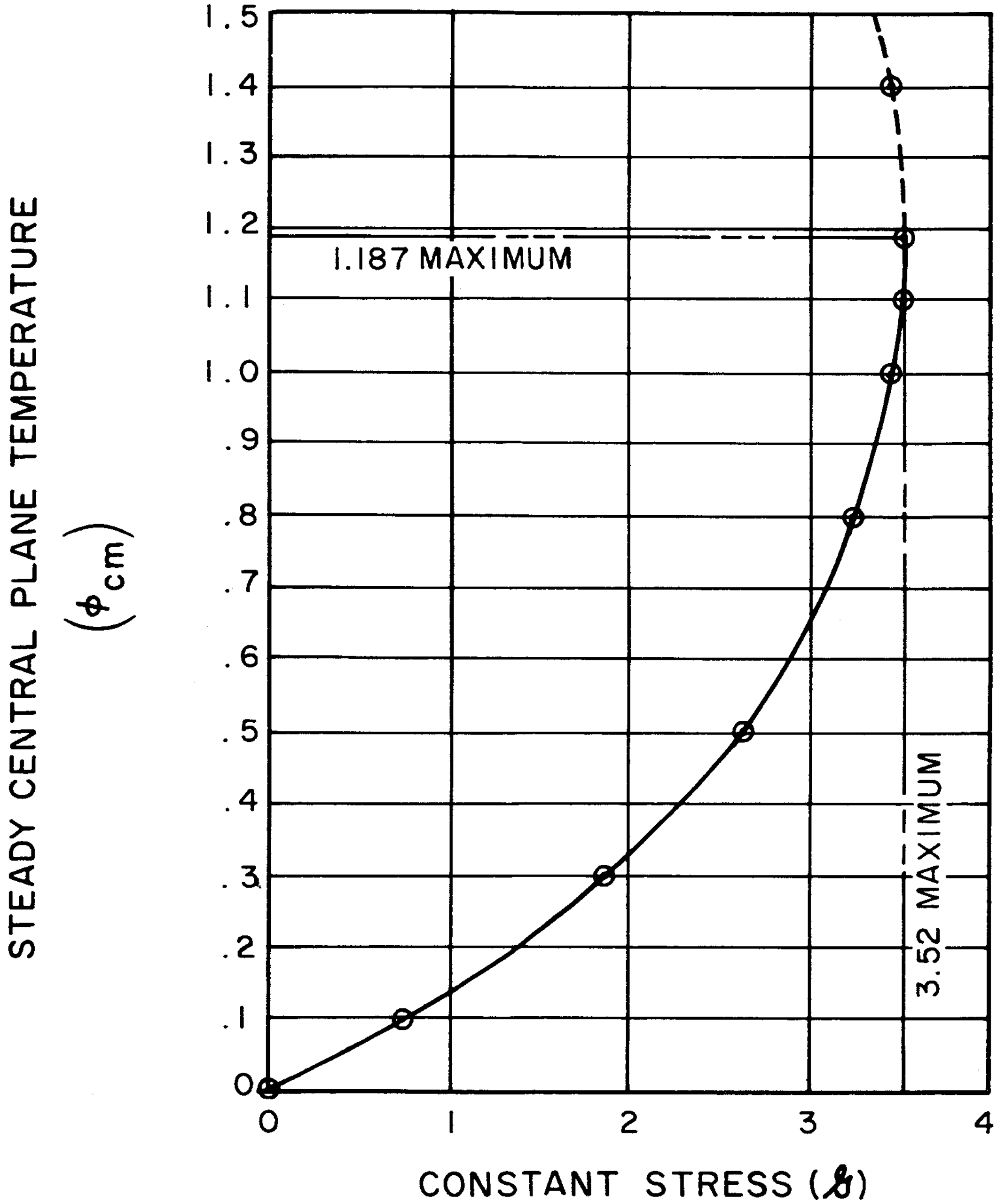

STEADY CENTRAL PLANE TEMPERATURE
(ϕ_{cm})
1.5
1.4
1.3
1.2
1.1
1.0
.9
.8
.7
.6
.5
.4
.3
.2
.1
0
1.187 MAXIMUM
3.52 MAXIMUM
0
1
2
3
4
CONSTANT STRESS ($\mathcal{S}$)

FIG. 3

CONSTANT RATE OF STRESS INCREASE

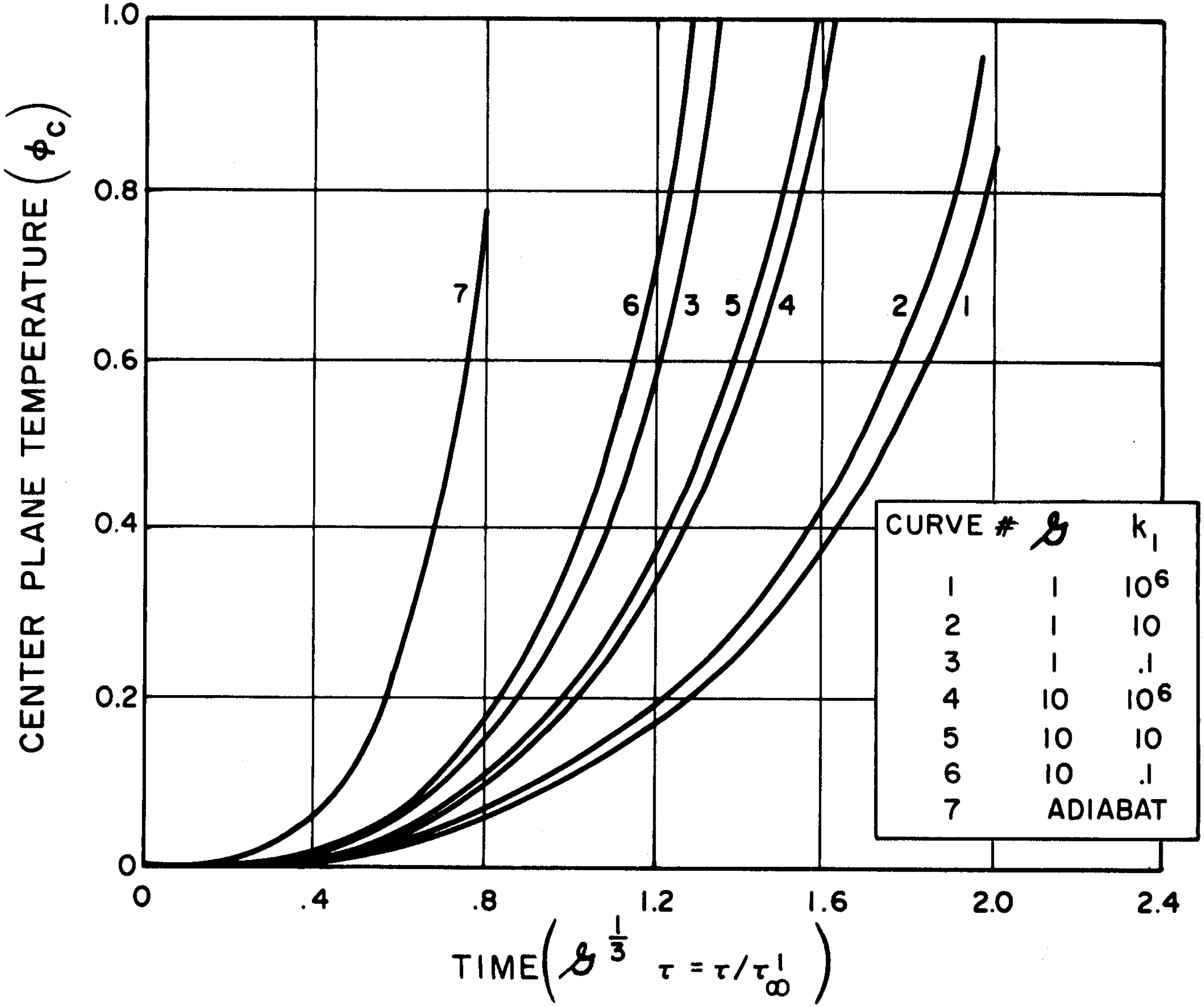

FIG. 4

CONSTANT RATE OF STRESS INCREASE

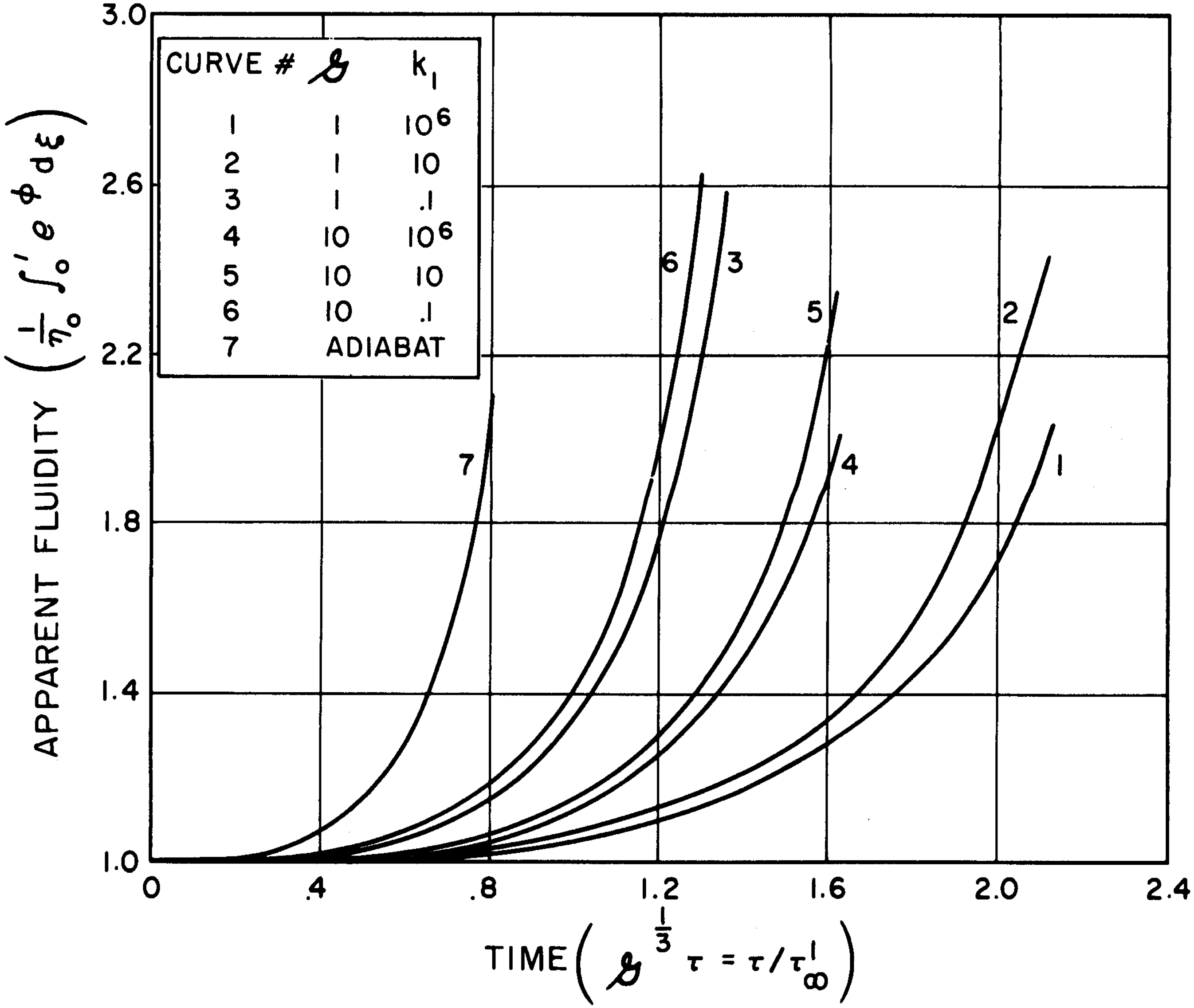

FIG. 5

CONSTANT DEFLECTION RATE

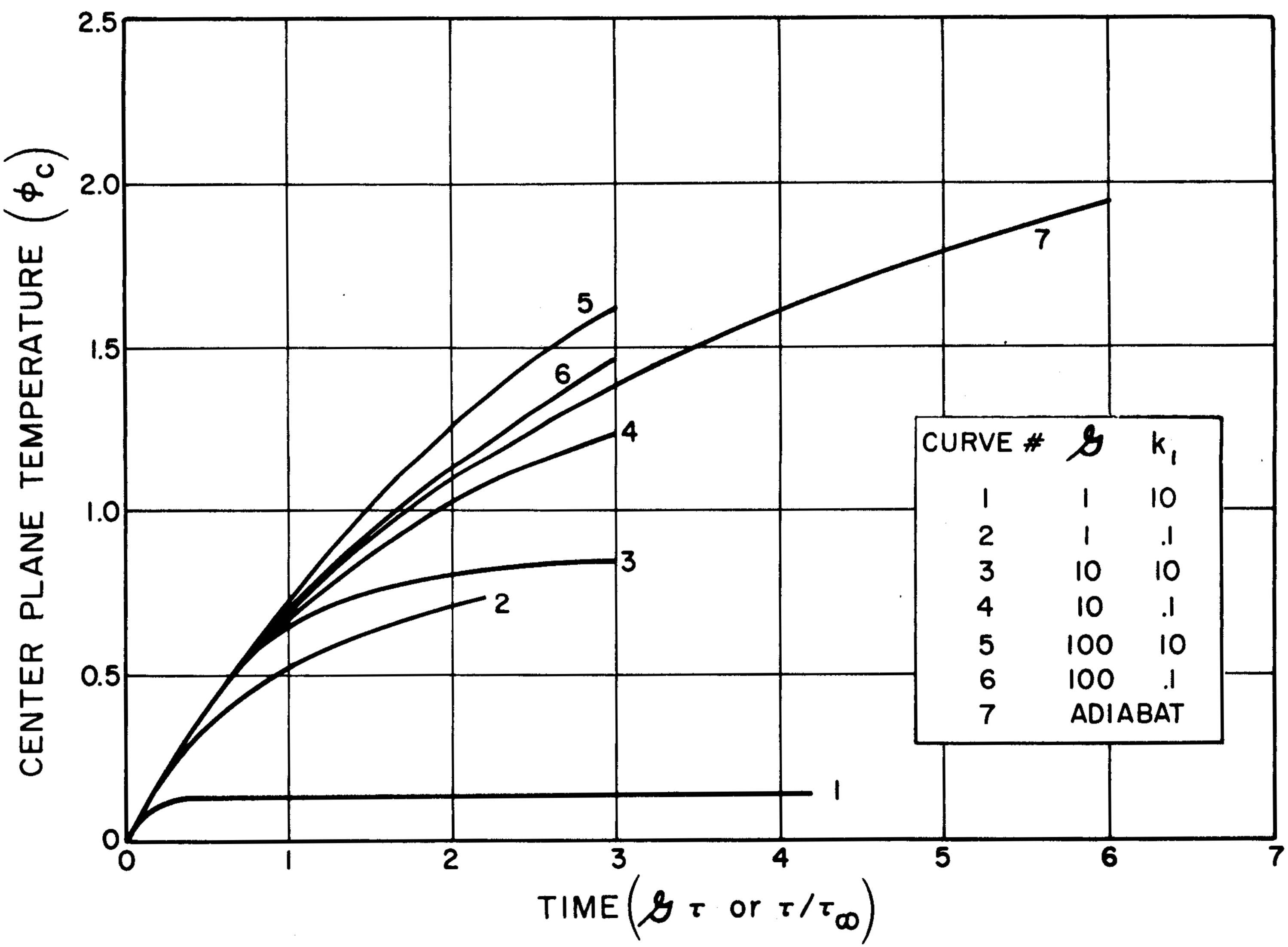

FIG. 6

CONSTANT DEFLECTION RATE

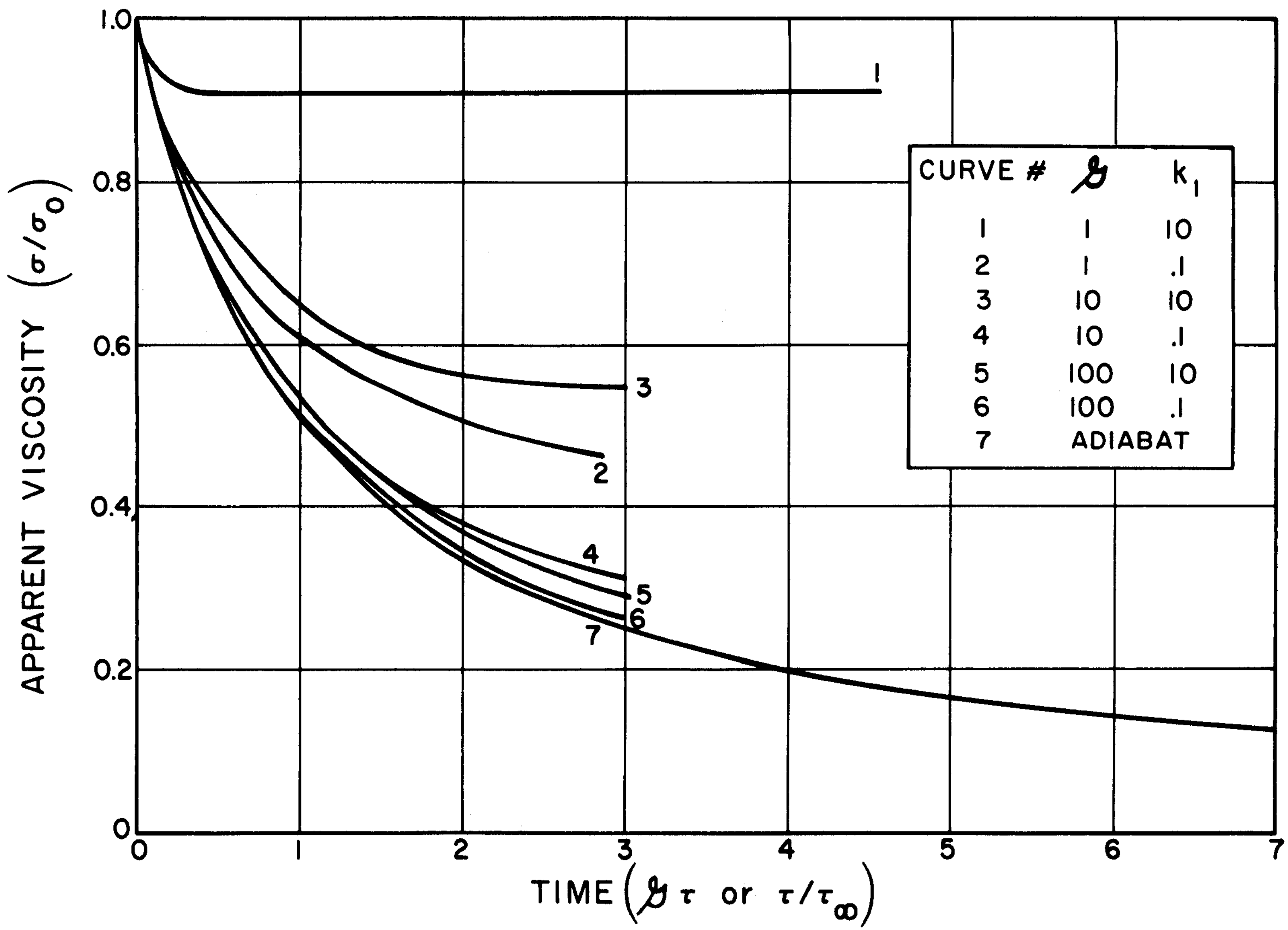

FIG. 7

EVOLUTION OF TEMPERATURE AND VELOCITY PROFILES FOR CONSTANT DEFLECTION RATE

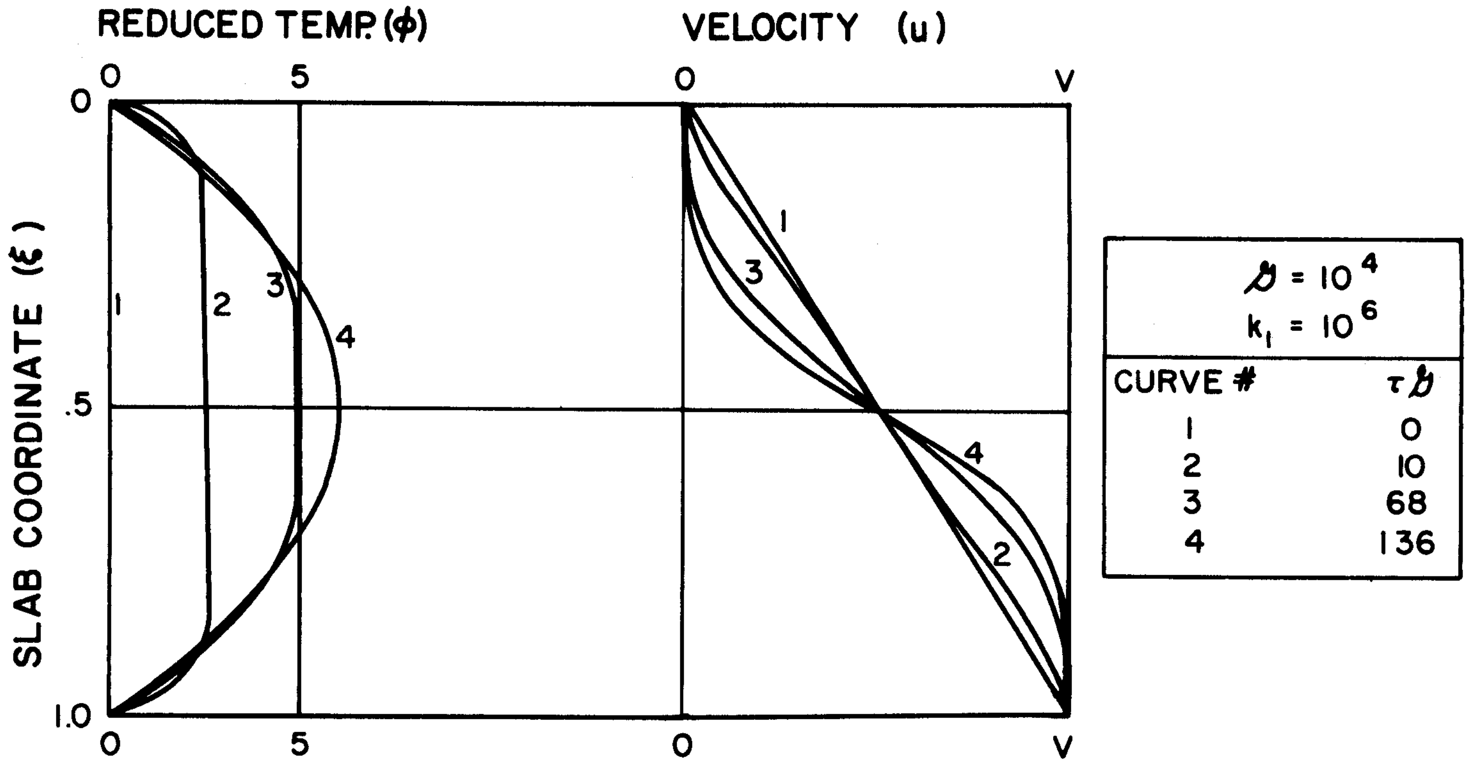

FIG. 8

THERMISTOR ANALOG OF VISCOSITY HYSTERESIS

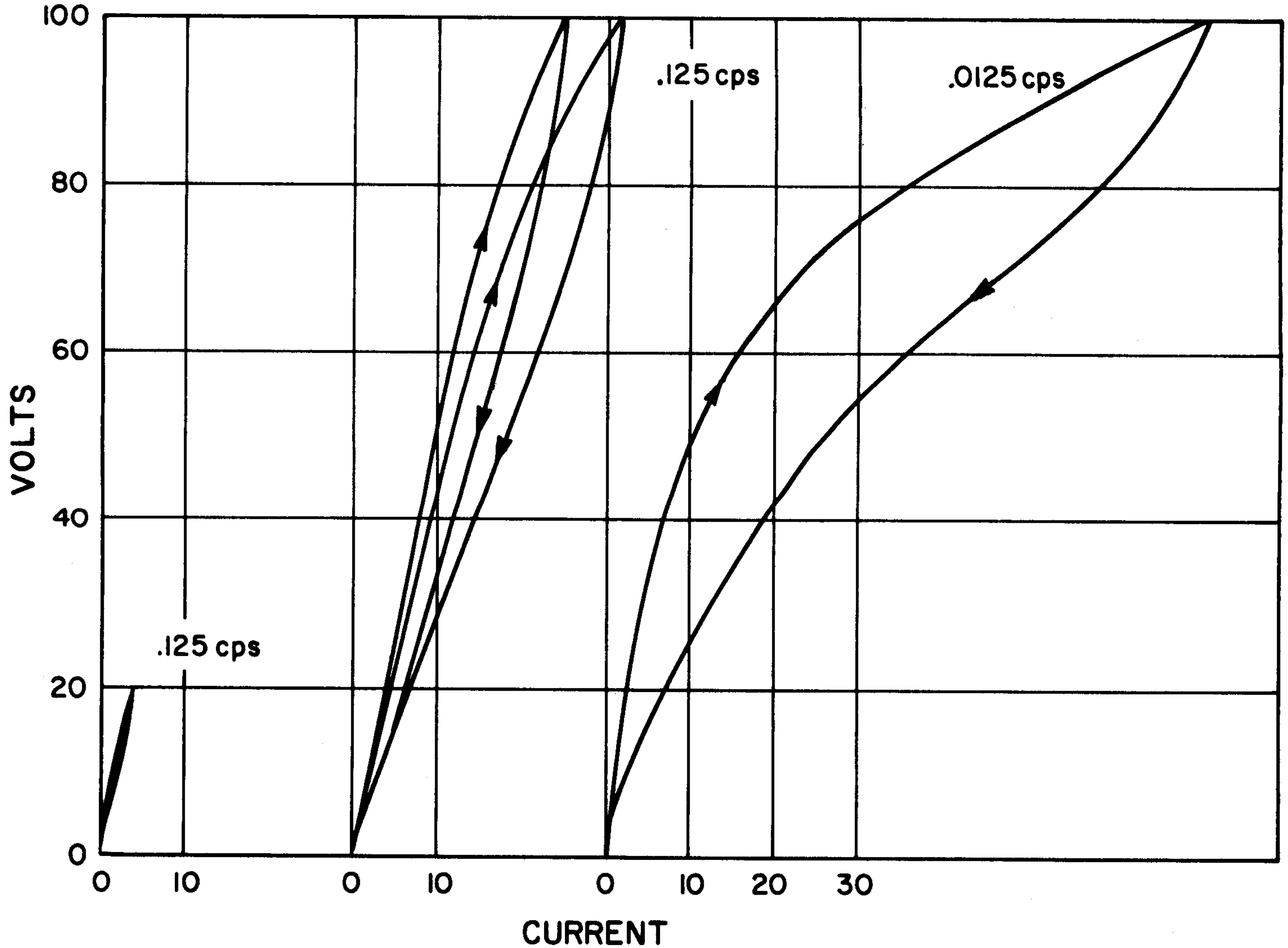

FIG. 9

N65 10678

THERMAL EFFECTS IN MODEL VISCOELASTIC SOLIDS

A Report proposed for presentation at the
6th Annual Structures and Materials Conference
American Institute of Aeronautics & Astronautics
Palm Springs, California
April, 1965

Prepared by:
I. J. Gruntfest and S. J. Becker
Re-entry Systems Department
General Electric Company
P. O. Box 8555
Phila.,Pa.
19101

June 1964

ABSTRACT

10678

As part of a general study of the behavior of materials with temperature dependent properties, a simple model of a viscoelastic solid is considered here. Ideal experiments at constant stress and constant rate of deformation are examined. The analysis leads to yield and fracture criteria which in the usual theory are regarded as experimentally determined quantities. Rate of strain and size effects are also deduced and a phenomenon resembling strain hardening can develop. The treatment is independent of, but complementary to, the atomic scale theories of the deformation of solids. The temperature coefficient of viscosity which is introduced into the continuum theory, here, is related to the energy of activation for the flow process which is accessible to the atomic scale theory. The appreciation of the temperature field in which motions of the atoms occur could improve the predictions based on dislocation theory.

Author

NOTATION

a - temperature coefficient of the viscosity of the working material.

c - the temperature independent, volumetric heat capacity of the working material.

g - a convenient non-dimensional group of parameters, or similarity criterion, which defines the initial source strength in the reduced energy equation.

k - the temperature independent volumetric thermal conductivity of the working material.

k_1 - the thermal conductivity of the insulation used to regulate the thermal boundary conditions relative to that of the working material.

ℓ - the thickness of the slab of material.

r - the deformation rate in the constant rate of deformation case.

t - current real time.

T - current local temperature.

T_0 - an initial or reference temperature.

u - the local velocity in the material relative to that at $\xi = 0$.

y - the space coordinate in the slab.

ϵ - the relative current boundary displacement of the slab of material.

ϵ_m - the maximum or equilibrium displacement of the viscoelastic slab for a constant applied stress.

η - the temperature dependent local viscosity in the viscous part of the viscoelastic model.

η_0 - the viscosity at the reference temperature.

μ - the spring constant in the elastic part of the viscoelastic model.

ξ - the reduced space variable.

σ - the current value of the shear stress on the viscous part of the model.

σ_0 - the initial value of the stress.

σ_E - the current stress on the elastic element in the constant rate of deformation case.

σ_T - the current value of the total stress in the constant rate of deformation case.

σ_V - the current stress on the viscous element in the constant rate of deformation case.

τ - the reduced time.

τ_m - the mechanical relaxation time; or the time at which the isothermal viscous stress has decayed to 1/e of its initial value.

τ_{∞} - the time at which the adiabatic stress has decayed to 1/2 its initial value in the constant rate of deformation case.

ϕ - the reduced temperature.

ϕ_{ℓ} - the critical temperature, characteristic of the material, at which fracture is expected.

ϕ_m - the maximum steady state value ϕ can reach.

ϕ_c - the reduced temperature on the center plane.

THERMAL EFFECTS IN MODEL VISCOELASTIC SOLIDS

INTRODUCTION

All mechanical processes involving real materials are to some extent irreversible and, therefore, must be accompanied by thermal effects. The irreversibility is complete in the flow of viscous fluids. The consequence of heat generation in one dimensional (Couette) flow of ideal viscous liquids have recently been explored (1). Criteria were established for estimating the significance of the heating effects which are useful for understanding apparent departures from Newtonian behavior.

In the present report, the exploration of the consequences of heating has been extended to include the deformations of model viscoelastic solids made by combining an ideal elastic element with the viscous model of reference 1. The use of such a model, or of any homogeneous isotropic, continuum model, ignores a great deal that is known about the physics of solids. However, it will be seen that this treatment is altogether complementary to the elegant and compelling atomic scale descriptions of the deformation of solids involving the theory of the imperfect crystal and the configurational changes of polymer molecules.

The existence of heating effects accompanying the deformation of solids has often been noted and is sometimes conspicuous (2) (3) (4) (5) (6). Because the deformations can be both exothermic and temperature sensitive, regenerative feedback can occur. This would enhance the thermal effects and could lead to instability. In the case of stressed liquid, the development of very high temperatures can be averted by convective circulations, turbulence and cavitation which consume large amounts of energy from the flow. In the case of solids, convective processes cannot occur, but thermal catastrophe can be averted by yielding and fracture.

When the temperature dependence of the viscous element is acknowledged, yield and fracture criteria follow as logical consequences. Rate of loading and size effects also appear in a natural manner and a phenomenon resembling strain hardening can develop. Furthermore, the introduction of the temperature coefficient of viscosity into the theory of the continuum, by itself, provides a bridge to the atomic scale events through the concept of the energy of activation.

While the results of this study of the continuum model are of intrinsic interest, the importance of this point of view is likely to be greater when it is used to supplement the solid state physics approach to the problem of deformation. With an appreciation of the temperature field in which atomic scale movements occur, the microscopic theory can be sharpened and, hopefully, better correlations with experiment will be obtained.

DISCUSSION OF ANALYSIS

In the analysis given below, the responses of a simple parallel arrangement of an ideal elastic element and an ideal viscous element to a constant stress and to a constant rate of deformation are examined. The idealizations that are made are that the spring constant, the heat capacity, the thermal conductivity and the density are independent of temperature. In addition, dynamic effects are neglected. Furthermore, the problem of shape changes accompanying the deformations is avoided by considering only plane shears in an infinite slab or, equivalently, torsion in a thin-walled tube.

The deformations are measured by the relative parallel displacements of the boundaries of the slab. The restraints are the shear displacement dependent elastic forces and displacement rate dependent viscous forces. The viscous forces are computed from the solutions of approximate energy and momentum equations as in reference 1.

Even with the above simplifications, the problem with heat generation and heat conduction is somewhat involved and unfamiliar. To assist in the interpretation of the numerical results obtained using an IBM 7094 computer, comparisons are made with the familiar isothermal and with the simple adiabatic behavior of the model.

In this model, the displacement of the two elements are always identical. The instantaneous value of the shear stress on the viscous element, σ , is related to the total stress, σ_T , by

$$\sigma = \sigma_T - \frac{\mu \epsilon}{\ell} \quad (1)$$

in which μ is the spring constant, ϵ is the relative boundary displacement and ℓ is the thickness of the slab.

The displacement is related to the viscous stress history by the definition

$$\epsilon = \int_0^t \int_0^\ell \frac{du}{dy}\, dy\, dt \tag{2}$$

in which y is the space variable, u is the local velocity relative to the boundary at y = 0, and t is the current time.

The application of the Newtonian viscosity law with exponentially dependent viscosity (see ref. 1)

$$\sigma = \eta \frac{du}{dy} = \eta_0 \frac{du}{dy} e^{-a(T-T_0)} \tag{3}$$

then leads to

$$\epsilon = \frac{1}{\eta_0} \int_0^t \sigma \int_0^\ell e^{a(T-T_0)}\, dy\, dt \tag{4}$$

in which η_0 is the viscosity at the temperature T_0; η and T are the local, instantaneous values of the viscosity and temperature and a is the temperature coefficient of viscosity.

The instantaneous local temperature is computed from the approximate energy equation

$$\sigma \frac{du}{dy} = c \frac{\partial T}{\partial t} - k \frac{\partial^2 T}{\partial y^2} \tag{5}$$

in which c and k are the volumetric heat capacity and thermal conductivity respectively. The solution of equation 5 depends on the momentum equation (equation 3) and the thermal boundary conditions defined in terms of the relative thermal conductivity of layers of insulating material, k_1, encasing the slab of working material. In the illustrative examples, the thickness of each of these layers is assumed to be one third of the thickness of the slab, and their outer boundaries are held at the initial temperatures.

Using reduced variables as in reference 1,

$$\phi = a(T - T_0), \quad \xi = \frac{y}{l}, \quad \tau = \frac{k}{c l^2} t \tag{6}$$

equation 5 becomes

$$g \left(\frac{\sigma}{\sigma_0}\right)^2 e^{\phi} = \frac{\partial \phi}{\partial \tau} - \frac{\partial^2 \phi}{\partial \xi} \tag{7}$$

in which

$$g = \frac{a \sigma_0^2 l^2}{k \eta_0} \tag{8}$$

Equation 4 becomes

$$\frac{\epsilon}{l} = \frac{c l^2}{k \eta_0} \int_0^{\tau} \sigma \int_0^{1} e^{\phi} \, d\xi \, d\tau \tag{9}$$

and equation 1 can be written

$$\sigma = \sigma_T - \frac{\mu c l^2}{k \eta_0} \int_0^{\tau} \sigma \int_0^{1} e^{\phi} \, d\xi \, d\tau \tag{10}$$

CREEP

If at $\tau = 0$, a total stress, σ_0 , is applied to the parallel arrangement of the elastic and viscous elements and held constant, equation 10 shows that the stress on the viscous element will have the initial value $\sigma = \sigma_T = \sigma_0$. At later times, $\sigma < \sigma_0$ and an equation for σ can be obtained from equation 10 by differentia- t ion with respect to time to get

$$\frac{d\sigma}{d\tau} = -\frac{c\mu l^2}{k\eta_0}\sigma\int_0^1 e^{\phi}\,d\xi \tag{11}$$

which upon separation of variables and integration gives

$$\frac{\sigma}{\sigma_0} = e^{-\frac{c\mu l^2}{k\eta_0}\int_0^{\tau}\int_0^1 e^{\phi}\,d\xi\,d\tau} \tag{12}$$

This can be substituted into equation 7 to give

$$y\,e^{\left(\phi - \frac{2}{\tau_m}\int_0^{\tau}\int_0^1 e^{\phi}\,d\xi\,d\tau\right)} = \frac{\partial\phi}{\partial\tau} - \frac{\partial^2\phi}{\partial\xi^2} \tag{13}$$

in which

$$\tau_m = \frac{k\eta_0}{c\mu l^2} \tag{14}$$

which together with appropriate thermal boundary conditions can be solved numerically. The results are described in a later section of this report.

In order to facilitate the understanding of the general numerical solutions of the creep equation, it is useful to inspect the ideal isothermal behavior of the model. In this case, e^{ϕ} in equation 12 is independent of ξ and equal to one. Thus, equation 12 becomes

$$\frac{\sigma}{\sigma_0} = e^{-\frac{\tau}{\tau_m}} \tag{15}$$

so that the stress on the viscous element and thus, the rate of displacement, decays to zero at a rate determined by the mechanical relaxation time, τ_m.

The instantaneous displacement for the isothermal case; from equation 1, can be written

$$\epsilon = \frac{l(\sigma_0 - \sigma_x)}{\mu} = \epsilon_m\left(1 - e^{-\frac{\tau}{\tau_m}}\right) \tag{16}$$

in which $\epsilon_m = \frac{\sigma_0 l}{\mu}$ is the maximum or equilibrium displacement. These results, familiar to rheologists, are plotted together with the solutions using equation 7 whenever they are appropriate.

An appreciation of the ideal adiabatic creep behavior of the model can also contribute to the understanding of the general numerical solutions of the creep equation. The development of the equations for the adiabatic case is somewhat more complicated and less familiar than the isothermal case.

Here e^{ϕ} is also independent of ξ so that equation 11 becomes

$$\frac{d\sigma}{d\tau} = -\frac{c\mu l^2}{K\eta_0}\sigma e^{\phi} \tag{17}$$

A value of e^{ϕ} can now be obtained from the adiabatic form of equation 7

$$y\left(\frac{\sigma}{\sigma_0}\right)^2 e^{\phi} = \frac{d\phi}{d\tau} \tag{18}$$

which can be substituted into equation 17 to give

$$\frac{d\sigma}{d\tau} = -\frac{\sigma}{\tau_m}\left(\frac{\sigma_0}{\sigma}\right)^2 \frac{1}{y} \frac{d\phi}{d\tau} \tag{19}$$

Separating variables and integrating leads to the relationship between the temperature and the stress on the viscous element

$$\sigma_0^2 - \sigma^2 = \frac{2\sigma_0^2}{\tau_m y} \phi \tag{20}$$

since $\phi = 0$ when $\sigma = \sigma_0$.

Notice that when $\sigma = 0$, ϕ reaches its maximum value so

$$\phi_m = \frac{y\tau_m}{2} \tag{21}$$

The solution can now be completed by substituting from equation 20 into 18 using 21 leading to

$$\frac{d\phi}{d\tau} = y\left(1 - \frac{\phi}{\phi_m}\right)e^{\phi} \tag{22}$$

Here the variables can be separated and we have

$$\int_0^{\phi} \frac{e^{-\phi}\, d\phi}{1 - \phi/\phi_m} = y\tau \tag{23}$$

or

$$\frac{\phi_m}{y}\int_0^{\phi} \frac{e^{-\phi}\, d\phi}{\phi_m - \phi} = \tau = \frac{\tau_m}{2}\int_0^{\phi} \frac{e^{-\phi}}{\phi_m - \phi}\, d\phi \tag{24}$$

The integral in equation 24 can be converted to a well-known tabulated function (the exponential integral, $Ei(z)$) by the substitution

$$z = \phi_m - \phi$$
$$dz = -d\phi \qquad (25)$$
$$e^z = e^{\phi_m} e^{-\phi}$$

whence

$$\tau = \frac{\tau_m}{2} e^{-\phi_m} \int_{\phi_m-\phi}^{\phi_m} \frac{e^z}{z} dz \qquad (26)$$

So that the adiabatic time temperature relation is

$$\tau = \frac{\tau_m}{2} e^{-\phi_m} \left[Ei(\phi_m) - Ei(\phi_m - \phi) \right] \qquad (27)$$

The adiabatic displacement history can be obtained from equation 20, 21 and 1.

$$\epsilon = \frac{(\sigma_0 - \sigma)l}{\mu} = l\left[\frac{\sigma_0}{\mu} - \frac{1}{\mu}\sqrt{\sigma_0^2 - \frac{2\sigma_0^2}{\tau_m a_y}\phi}\right] \qquad (28)$$
$$= \epsilon_m \left(1 - \sqrt{1 - \phi/\phi_m}\right)$$

The adiabatic creep deformation history of the model, computed as indicated above using tables of $Ei(z)$, is compared with the more familiar isothermal deformation history in figure 1. Notice that if the value of ϕ_m is small ($\phi_m < 0.1$) the adiabatic and isothermal curves are quite close together. As ϕ_m increases, the approach to ϵ_m is much more rapid in the adiabatic case.

The adiabatic creep temperature history is plotted in figure 2. The use of ϕ/ϕ_m as a temperature scale tends to exaggerate the temperature effects at low ϕ_m and contracts them at high values of ϕ_m.

A graphical representation of the adiabatic creep displacement — temperature relationship (equation 28) is given in figure 3 together with a curve for a case with heat conduction. The point of this figure is that while in the adiabatic case the temperature reaches its maximum when the strain reaches its maximum, in the real case the rate of heat generation becomes so slow when ϵ approaches ϵ_m that the conduction process can cause the temperature to fall.

The description of the creep behavior of the model with both heat generation and heat conduction cannot be discussed (except qualitatively) without the numerical solutions of equation 11. The machine solutions for the deformation history for various values of ϕ_m and k_1 are presented in figures 3 and 4. The computed values of the temperature on the center plane of the viscous element for $\phi_m = 2.5$ and 25 for various values of k_1 are shown in figures 5 and 6.

This model is only suitable for describing what has been called primary creep (7). Secondary creep can be better described in terms of the viscous element by itself as is mentioned in reference 1. The duration of the primary creep phase is regulated by the value of ϕ_m, τ_m and the thermal boundary conditions. Another matter is the question of whether the material will survive the primary creep phase. If the temperature attained in the sample exceeds some critical value characteristic of the material, say ϕ_l, fracture can be expected before primary creep is complete. Obviously, this cannot happen if $\phi_m < \phi_l$.

However, even if $\phi_m > \phi_\ell$, fracture need not occur if the thermal boundary conditions are such as to prevent ϕ from exceeding ϕ_ℓ .

Another example of the type of experiment to which these computations would be applicable are, perhaps, those relating to the shear strength of adhesive or brazed joints. There have been many studies which have shown that thin joints can be stronger than thick joints as predicted by the analysis (8) (9).

CONSTANT RATE OF RELATIVE BOUNDARY DISPLACEMENT

When the model solid consisting of a simple elastic element and a simple viscous element in parallel is deformed at a constant rate, $\epsilon = rt$, the total stress is the sum of the independent stresses on each of the elements (equation 1). Although this "experiment" is more complicated, in principle, than the creep experiment, it is more commonly used for the evaluation of the "properties" of solids. Here, the problem of the instantaneous application of a stress does not arise. Furthermore, by the regulation of the deformation rate, the time required for the completion of a test can be varied over a wide range. This experiment is always terminated by yield or fracture. Thus, it provides a value of the "strength" of the material.

In this experiment, the stress on the elastic element increases linearly with time according to

$$\sigma_\epsilon = \frac{\mu \epsilon}{\ell} = \frac{\mu r t}{\ell} = \frac{c \mu \ell r \tau}{k} \qquad (29)$$

The stress on the viscous element deformed at a constant rate is somewhat more complicated. This matter was discussed in detail in reference 1 where it was shown that

$$\sigma_v = \frac{\eta_0}{\ell} r \left[\int_0^1 e^{\phi} d\xi \right]^{-1} = \sigma_0 \left[\int_0^1 e^{\phi} d\xi \right]^{-1} \tag{30}$$

so that the total stress obtained by combining equations 29 and 30 becomes

$$\sigma_T = \frac{c\mu \ell r \tau}{k} + \frac{\eta_0}{\ell} r \left[\int_0^1 e^{\phi} d\xi \right]^{-1} \tag{31}$$

The values of ϕ and the integral of e^{ϕ} then are obtained from the solutions of equation 7. Because of the independence of the viscous and elastic stresses, the numerical solutions of equation 7 presented in figures 6 and 7 of reference 1 and the discussion therein are directly applicable. However, before considering the significance of equation 31, the more familiar isothermal and adiabatic stress histories of the model will be examined.

If the temperature throughout the material always has the initial value, the value of the integral in equation 31 is unity. The viscous stress then has the constant value

$$\sigma_v = \frac{\eta_0}{\ell} r \tag{32}$$

and the total stress is given by

$$\sigma_T = \frac{c\mu \ell r \tau}{k} + \frac{\eta_0}{\ell} r \tag{33}$$

Thus, for the isothermal case, the relationship between the stress and the time (or deformation) can be represented by a straight line with the slope $\frac{c\mu \ell r}{k}$ and the intercept at $\tau = 0$ of $\frac{\eta_0}{\ell} r$. This is a relationship familiar to rheologists and it is shown together with examples of the adiabatic relationship in figure 8.

In the absence of heat conduction (adiabatic case) the value of ϕ is also independent of ξ, but the appropriate value of e^{ϕ} is given in reference 1 as

$$e^{\phi} = 1 + \frac{\tau}{\tau_\infty} \tag{34}$$

in which

$$\tau_\infty = \frac{k}{a\eta_0 r^2 \ell^2} \tag{35}$$

The adiabatic viscous stress is then time dependent according to

$$\sigma_v = \frac{\eta_0 r}{\ell} \frac{1}{1 + \tau/\tau_\infty} \tag{36}$$

Equation 31 for the total stress then has the form

$$\sigma_T = \frac{c\mu \ell r}{k} \tau + \frac{\eta_0 r}{\ell} \frac{1}{1 + \tau/\tau_\infty} \tag{37}$$

or

$$\sigma_T = \frac{\eta_0 r}{\ell} \left(\frac{\tau^2 + \tau_\infty \tau + \tau_\infty \tau_m}{\tau_m \tau + \tau_m \tau_\infty} \right) \tag{38}$$

While the first term of the expression on the right hand side of equation 37 increases linearly with deformation (or time) as before, the second term decreases. If this rate of decrease is high, the total stress can also decrease with deformation producing an effect similar to yield. On the other hand, the rise of the first term can arrest this decline and produce an effect similar to work hardening.

Examples of the adiabatic and isothermal relationships between total stress and deformation are plotted in figure 8 together with the curves for the separate elements of the composite model.

Returning now to the problem of the numerical solutions of equation 31 for the time (or deformation) dependent stress on the model subjected to a constant deformation rate, it is seen that the total stress is composed of that on the viscous element, already presented in reference 1, plus a linear term. In any particular situation, these terms can be assembled. The adiabatic curves shown in figure 8 are typical.

It may be seen that when the value of τ_∞ is low, a high initial stress and a pronounced dip or yield can be expected. This is also the condition that leads to the rapid development of a high temperature in the material that could lead to failure at low values of the displacement (brittleness). If failure does not occur promptly, at yield, the stress can rise again before the "lethal" temperature is reached, thus producing the strain hardening effect. This analysis can also account for the strong dependence of yield on strain rate that has often been observed experimentally.

CONCLUDING DISCUSSION

The analysis of thermal effects in a model solid given above is part of a continuing study of the behavior of materials with temperature dependent properties. It explores the general consequences of the conservation of energy on mechanical behavior in a simple but fundamental manner. It is not intended to apply to any particular material but rather to display the potential of a somewhat different type of phenomenological description of deformation and fracture. The point of view is not altogether new. Zener (2) and others have remarked on adiabatic instability in deformation. Seitz (10) remarks on the possibility of regeneration in the movement of dislocations in metals. The essential novelty seems to be that the question of thermal feedback is the focal point of the present study.

The results teach that an extremely primitive model can account for a number of details of the behavior of real solids. In the traditional treatments which neglect thermal feedback, the processes of yield and fracture and their time and size dependencies require rather intricate rationalizations. The possibility of exchanging the usual yield and fracture criteria by some more basic notions of what controls the responses of materials to stress could be useful both in design problems and in materials development.

Of further interest is the possibility of strengthening the solid state physics approach to the deformation problem. From the atomic scale point of view, the energy of activation for the movement of dislocations, which appears directly in the temperature dependence of the process, is an accessible quantity. Thus, a new bridge over the gap between the atomic scale and continuum view of the mechanics of solids may be provided.

Finally, it may be noted that the discussion and analysis of reference 1 is a special viscoelastic case in which the elasticity is negligible. The importance of the elastic effect depends on the value of both $\mathcal{Y}$ and τ_m. Whenever τ_m is sufficiently small, the elastic effect is important. But even for τ_m small, if $\mathcal{Y}$ is sufficiently high the viscous ~~heating~~ effects dominate.

ACKNOWLEDGEMENT

The study program part of which has been discussed above has been made possible by the encouragement and support of the Office of Advanced Research and Technology of the National Aeronautics and Space Administration under Contract NASw 708 monitored by Messrs. Howard Wolko and Melvin Rosché. The authors are also indebted to their colleagues Paul Gordon, Charles Grebey and George Mueller for helpful discussions and assistance in performing the analyses and computations.

1. Gruntfest, I.J., "Apparent Departures from Newtonian Behavior in Liquids Caused by Viscous Heating", proposed for presentation at the 35th Annual Meeting, Society of Rheology (Oct., 1964).

2. Zener, C., "The Micro-mechanism of Fracture", Am. Society for Metals Seminar on "Fracturing of Metal", 1948 (Book),

3. Dillon, O.W., "Temperatures Generated in Aluminum Rods Undergoing Torsional Oscillations", Journal Applied Phys. 33, 3100-3105 (1962).

4. Schapery, R.A., "Effects of Cyclic Loading on the Temperature in Viscoelastic Media with Variable Properties", AIAA Journal 2, 827-835, May (1964).

5. Gruntfest, I.J., "A Note on Thermal Feedback and the Fracture of Solids", Chapter in Book "Fracture of Solids", edited by D.C. Drucker and J.J. Gilman, Interscience, N.Y. (1963) (pages 189-193).

6. Mueller, F.H. and Jackel, K., Kolloid Zeits, 129, 145-146 (1952).

7. Nadai, A., "The Theory of Flow and Fracture of Solids", McGraw-Hill, New York (1950) (page 25).

8. Mar, J.W., and Shepard, L.A., "Some Studies on the Nature of Deformation in Composite Materials", AIAA Paper #2924-63, presented at Palm Springs, Cal., April, 1963.

9. Bikerman, J.J., "The Rheology of Adhesion", article in book "Rheology" edited by F. R. Eirich, Academic Press, New York (1960).

10. Seitz, F., "The Physics of Metals", McGraw-Hill, New York (1943), page 141.

CAPTIONS FOR FIGURES

#1 The reduced, time dependent adiabatic creep deformation ($\frac{\epsilon}{\epsilon_m}$) for various values of the reduced maximum temperature ϕ_m.

#2 The reduced, time dependent adiabatic creep temperature (ϕ/ϕ_m) for various values of the reduced maximum temperature ϕ_m.

#3 The reduced temperature dependent creep deformation $(1-\frac{\epsilon}{\epsilon_m})^2$ for the adiabatic case and for a case with heat conduction ($y=5$, $\tau_m=1$, $k_1=10$)

#4 The reduced, time dependent creep deformation for $\phi_m = 2.5$ and for various thermal boundary conditions. ($y = 5$, $\tau_m = 1$).

#5 The reduced, time dependent creep deformation for $\phi_m = 25$ and for various thermal boundary conditions. ($y = 5$, $\tau_m = 10$).

#6 Detail near the origin of the reduced time dependent center plane temperature ϕ_c/ϕ_m for $y = 5$, $\tau_m = 1$, ($\phi_m = 2.5$) and for various thermal boundary conditions.

#7 Detail near the origin of the reduced time dependent center plane temperature ϕ_c/ϕ_m for $y = 5$, $\tau_m = 10$, ($\phi_m = 25$) and for various thermal boundary conditions.

#8 Examples of the relationship between the stress ($\frac{\sigma}{\sigma_0}$) and the time (or deformation) ($\frac{\tau}{\tau_m}$) for the constant rate of boundary displacement case.

ADIABATIC CREEP

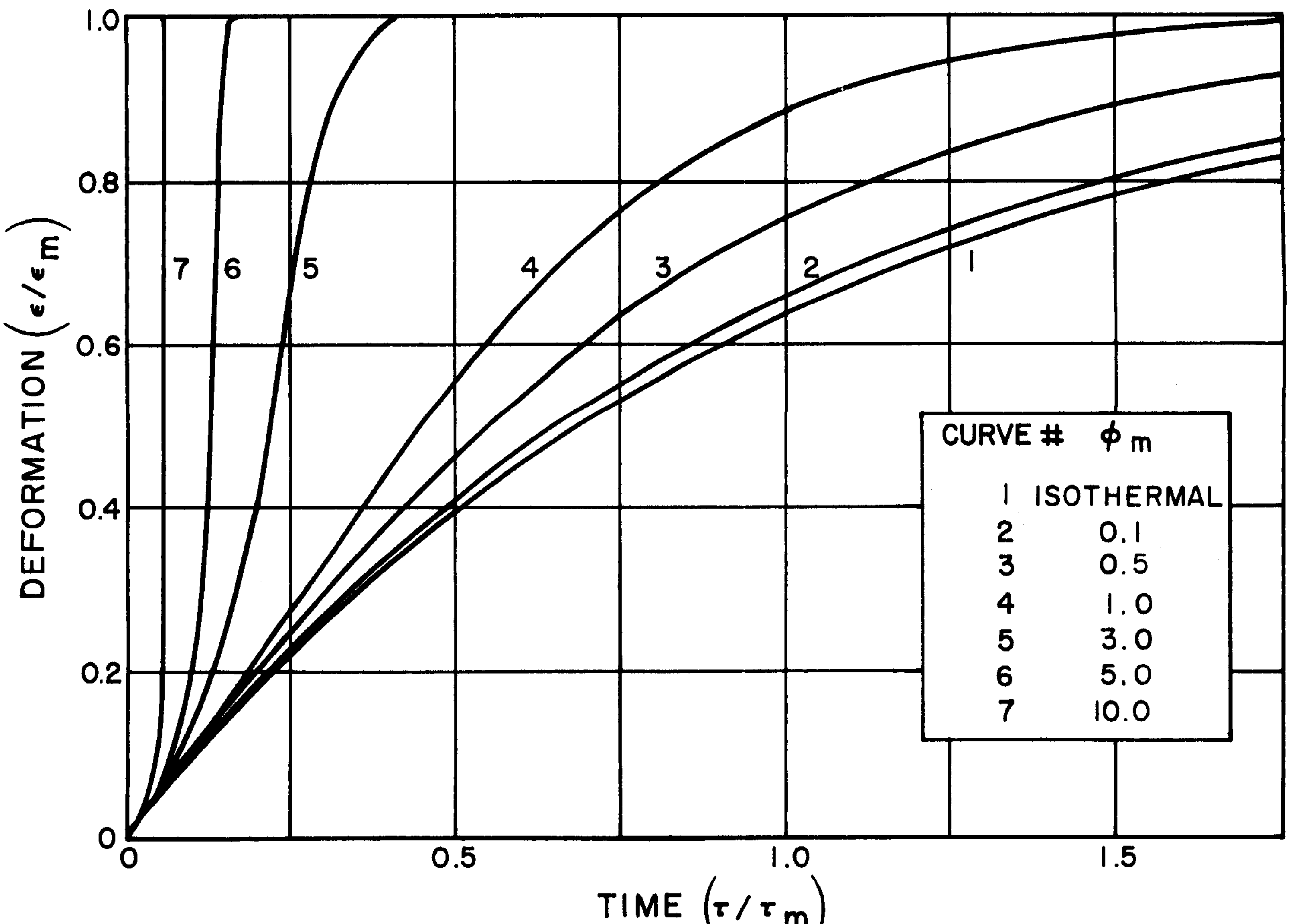

FIG. 1

ADIABATIC CREEP

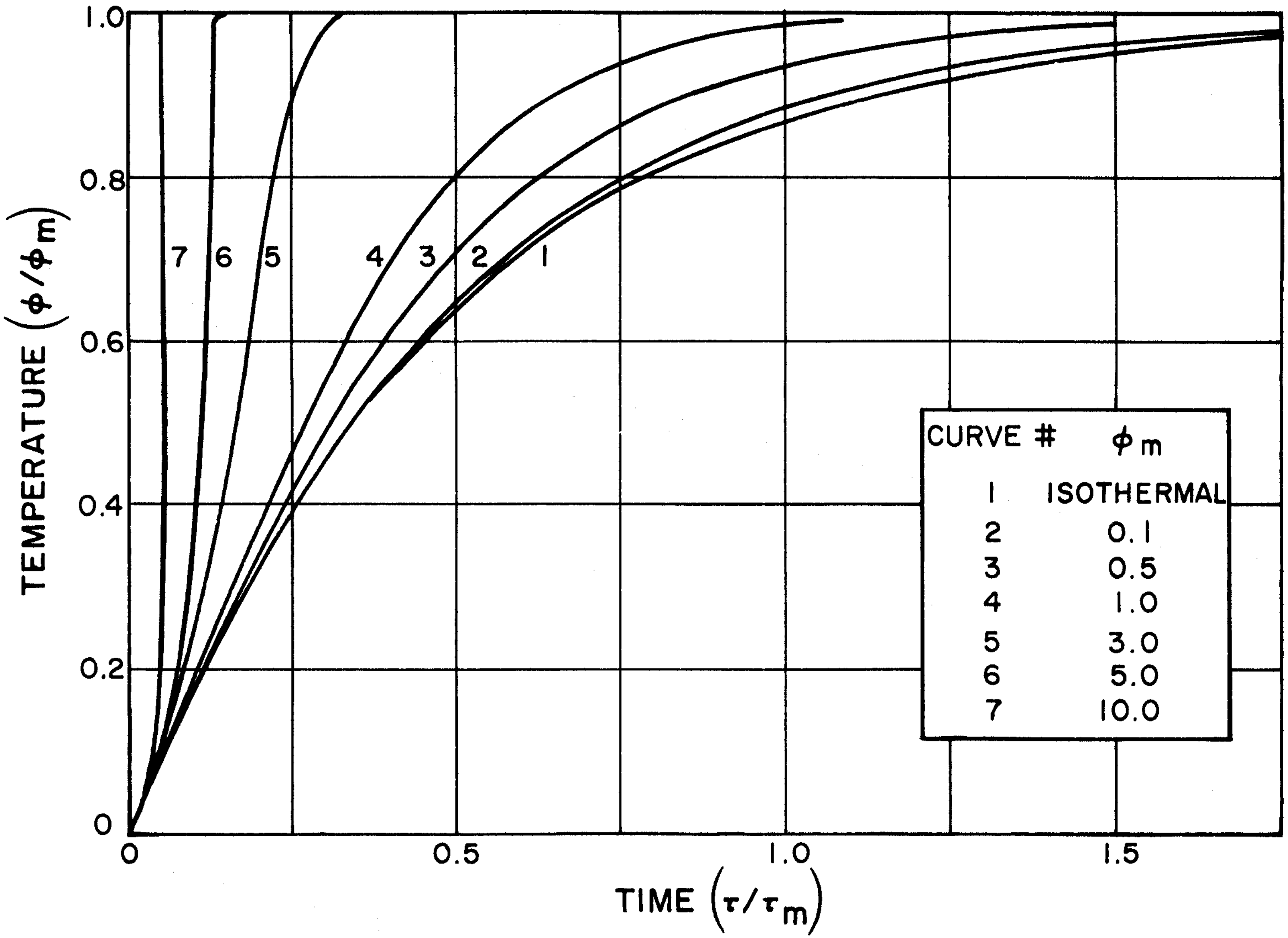

FIG. 2

CREEP

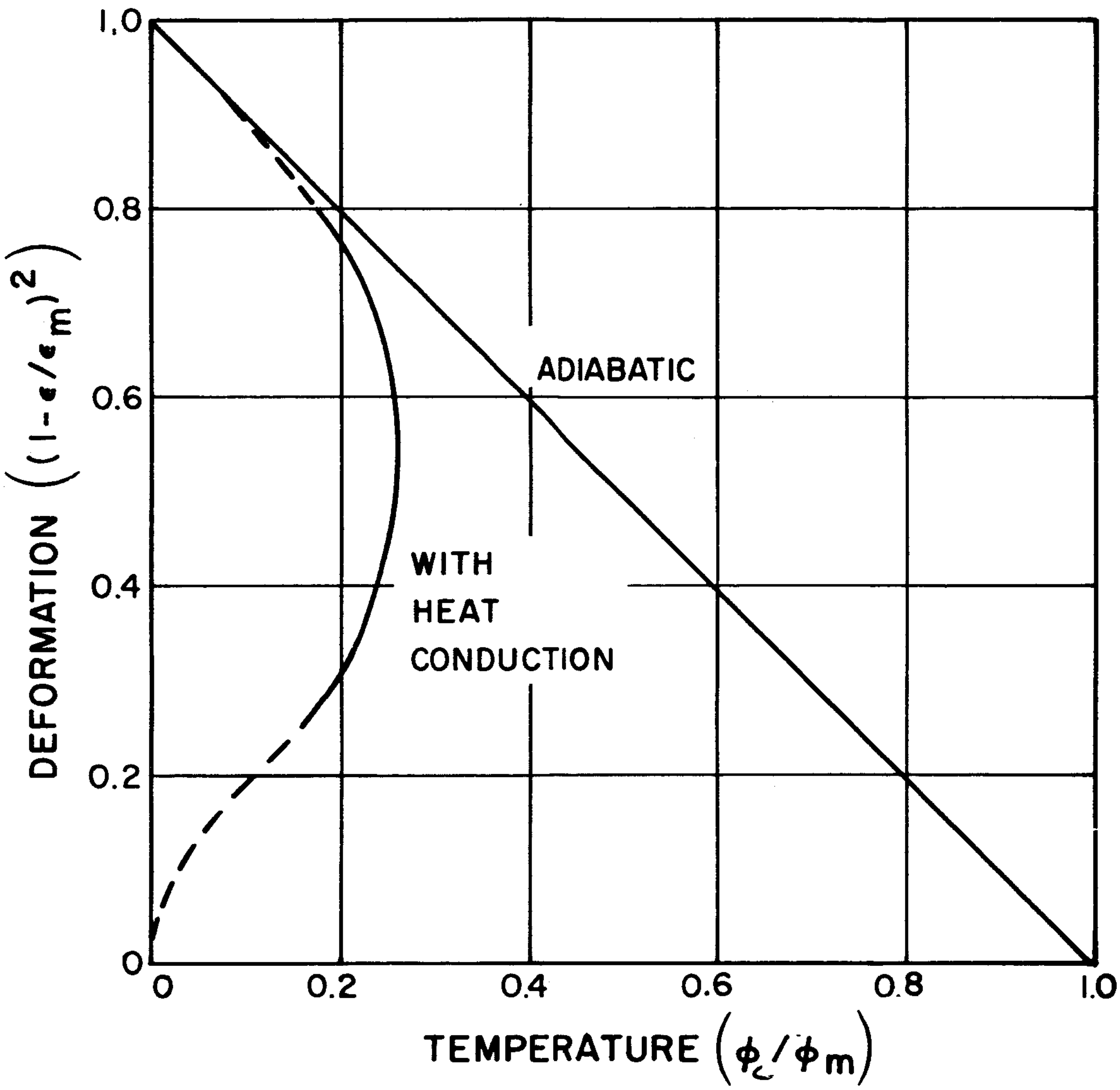
1.0
0.8
0.6
0.4
0.2
0
DEFORMATION $\left((1-\epsilon/\epsilon_m)^2 \right)$
ADIABATIC
WITH
HEAT
CONDUCTION
0
0.2
0.4
0.6
0.8
1.0
TEMPERATURE $\left(\phi_c/\phi_m \right)$

FIG. 3

CREEP

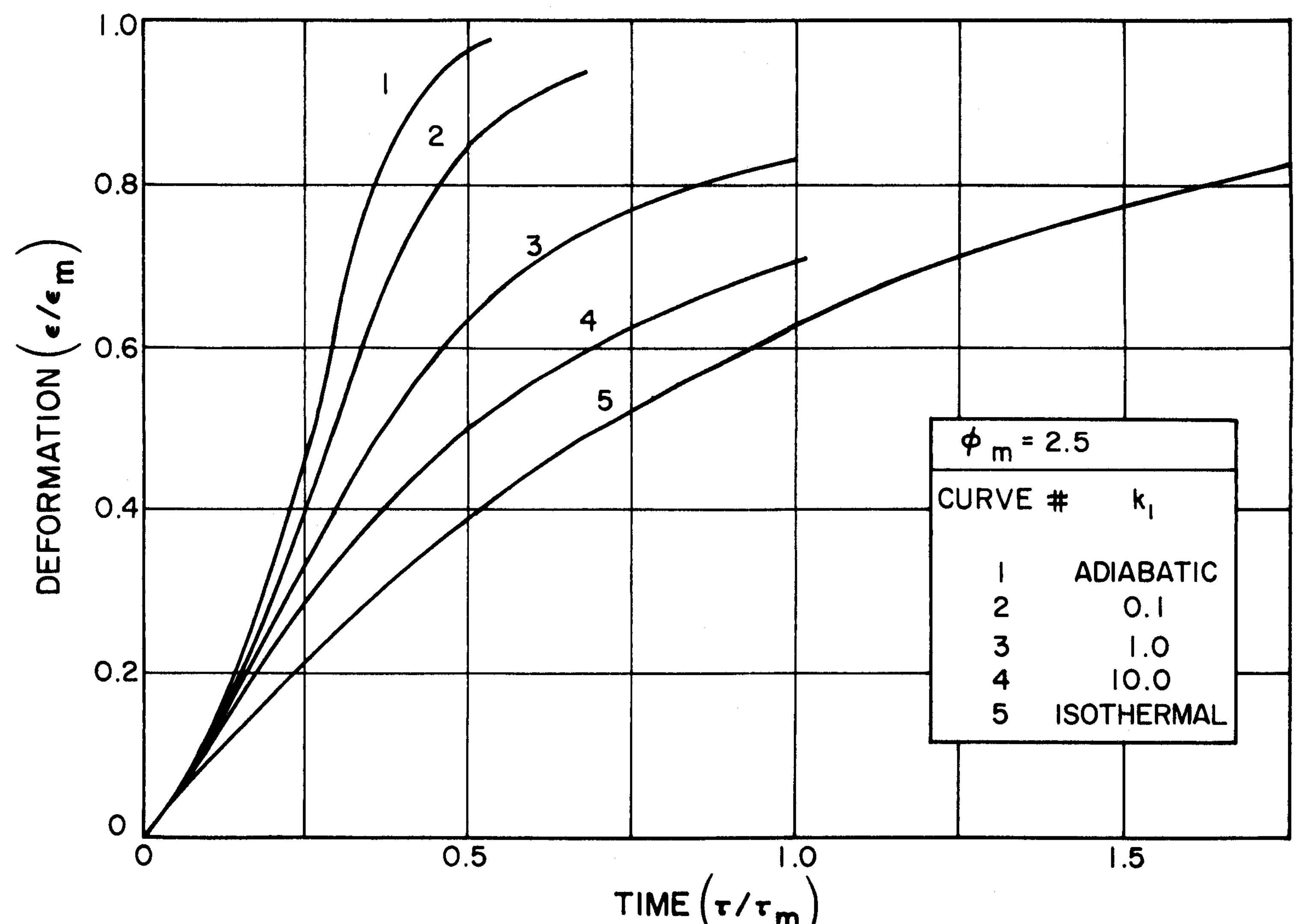
DEFORMATION (ϵ/ϵ_m)
1.0
0.8
0.6
0.4
0.2
0
0.5
1.0
1.5
1
2
3
4
5
$\phi_m = 2.5$
CURVE #
k_1
1 ADIABATIC
2 0.1
3 1.0
4 10.0
5 ISOTHERMAL
TIME (τ/τ_m)

FIG. 4

CREEP

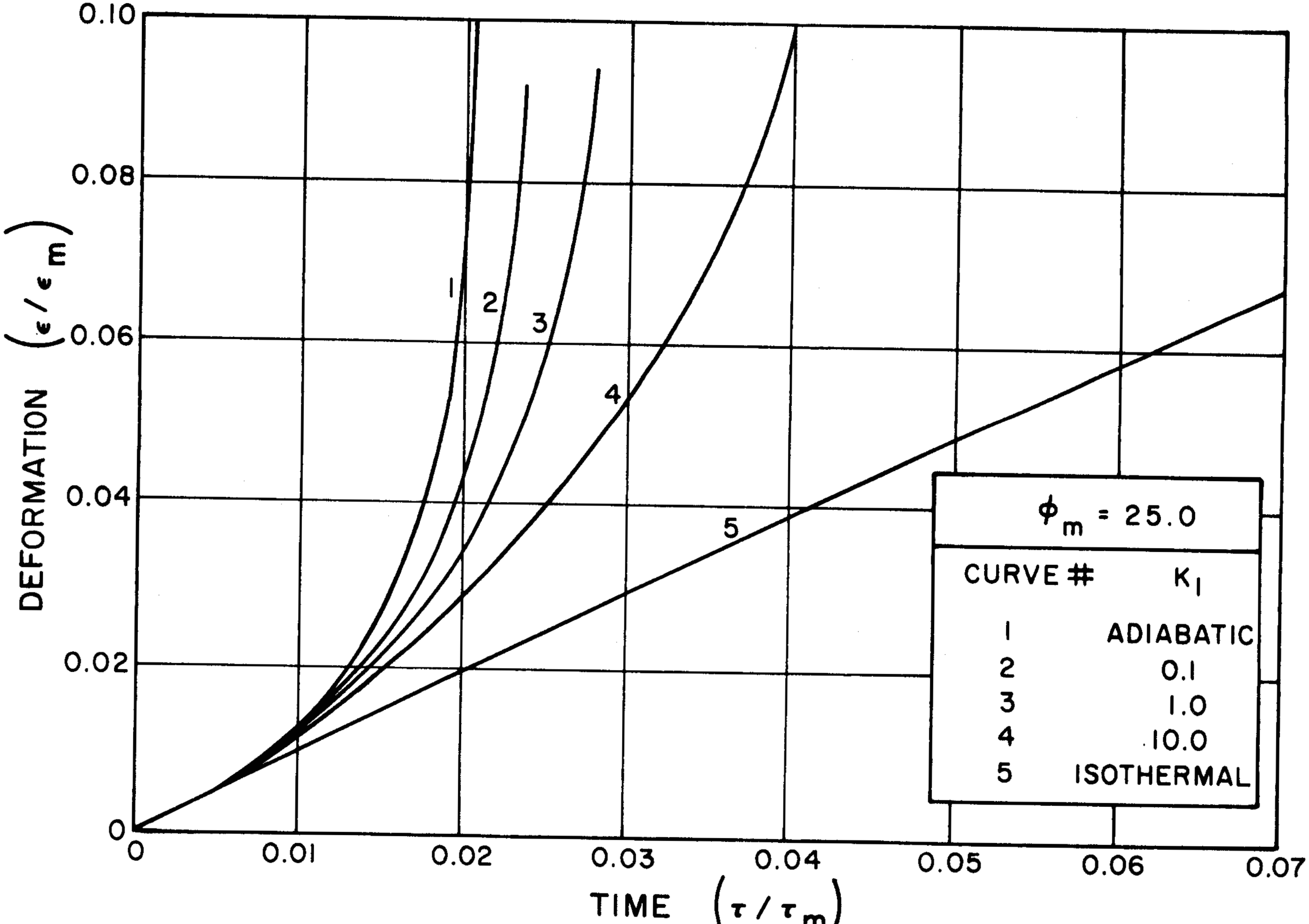
0.10
0.08
0.06
0.04
0.02
0
DEFORMATION (ϵ / ϵ_m)
0
0.01
0.02
0.03
0.04
0.05
0.06
0.07
TIME (τ / τ_m)
1
2
3
4
5
$\phi_m = 25.0$
CURVE # K_1
1 ADIABATIC
2 0.1
3 1.0
4 10.0
5 ISOTHERMAL

FIG. 5

CREEP

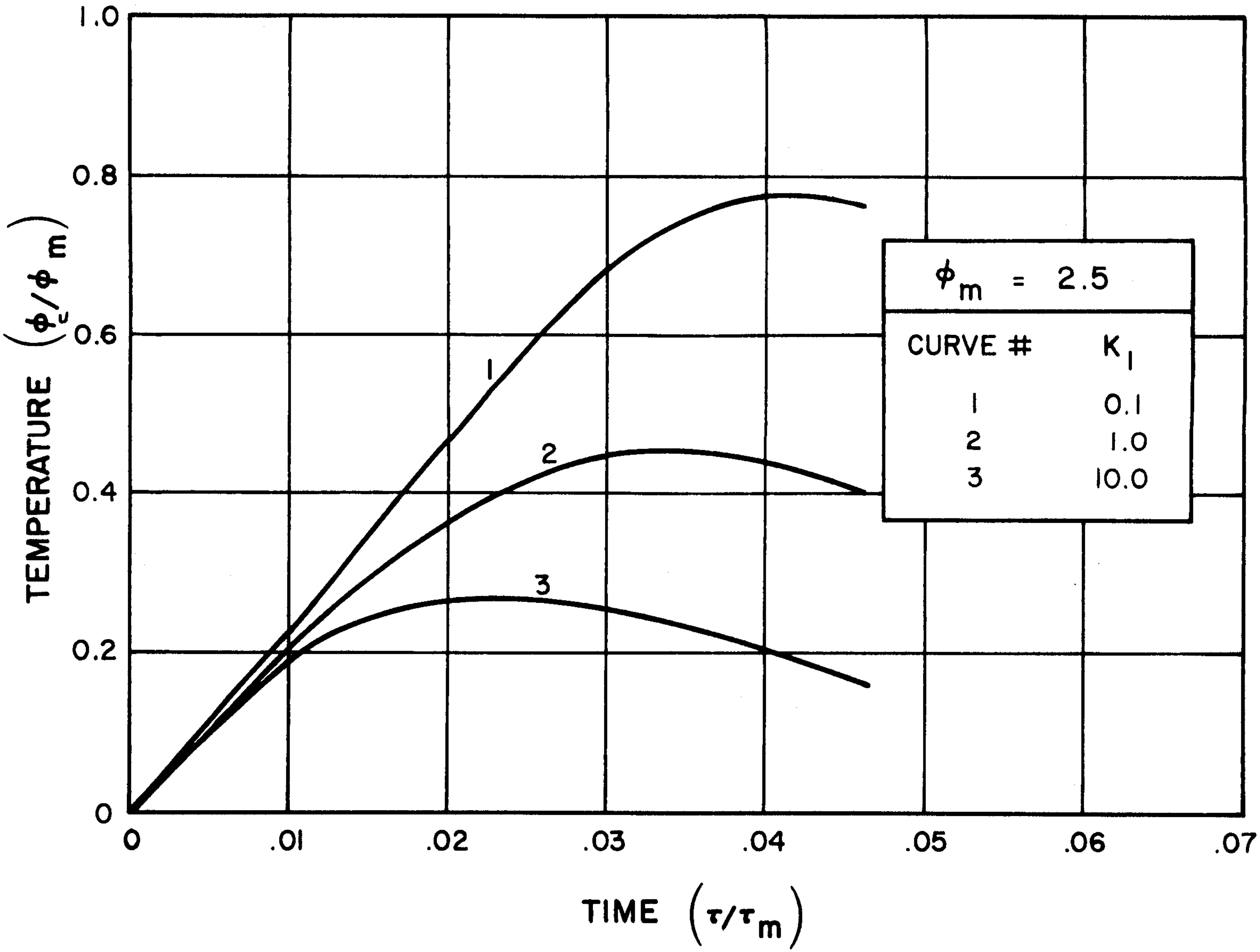

1.0
0.8
0.6
0.4
0.2
0
TEMPERATURE (ϕ_c/ϕ_m)
0
.01
.02
.03
.04
.05
.06
.07
TIME (τ/τ_m)
1
2
3
ϕ_m = 2.5
CURVE #
K_1
1
0.1
2
1.0
3
10.0

FIG. 6

CREEP

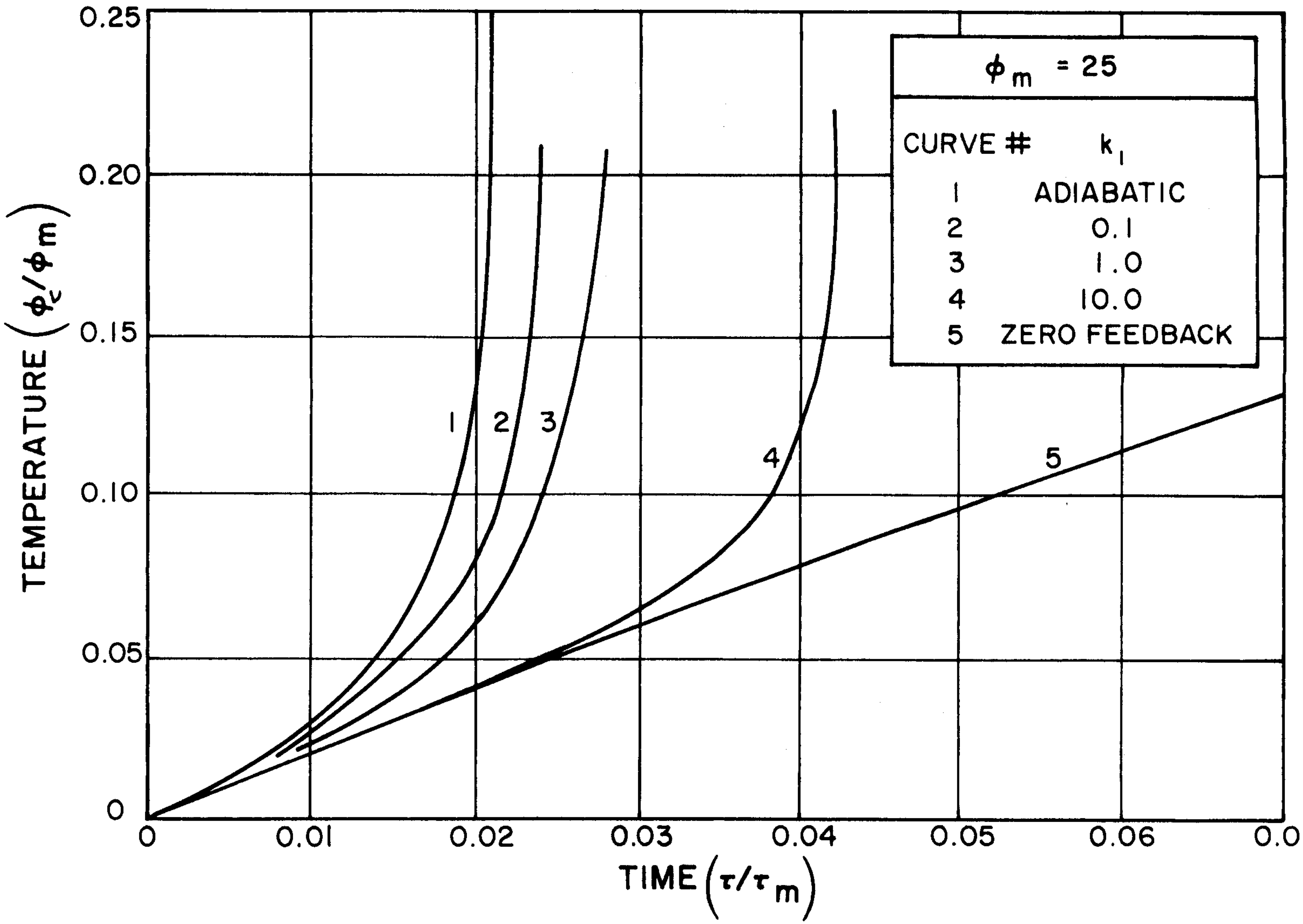

0.25
0.20
0.15
0.10
0.05
0
TEMPERATURE (ϕ_c/ϕ_m)
0
0.01
0.02
0.03
0.04
0.05
0.06
0.07
TIME (τ/τ_m)
ϕ_m = 25
CURVE # k_1
1 ADIABATIC
2 0.1
3 1.0
4 10.0
5 ZERO FEEDBACK
1
2
3
4
5

FIG. 7

CONSTANT RATE OF DEFORMATION

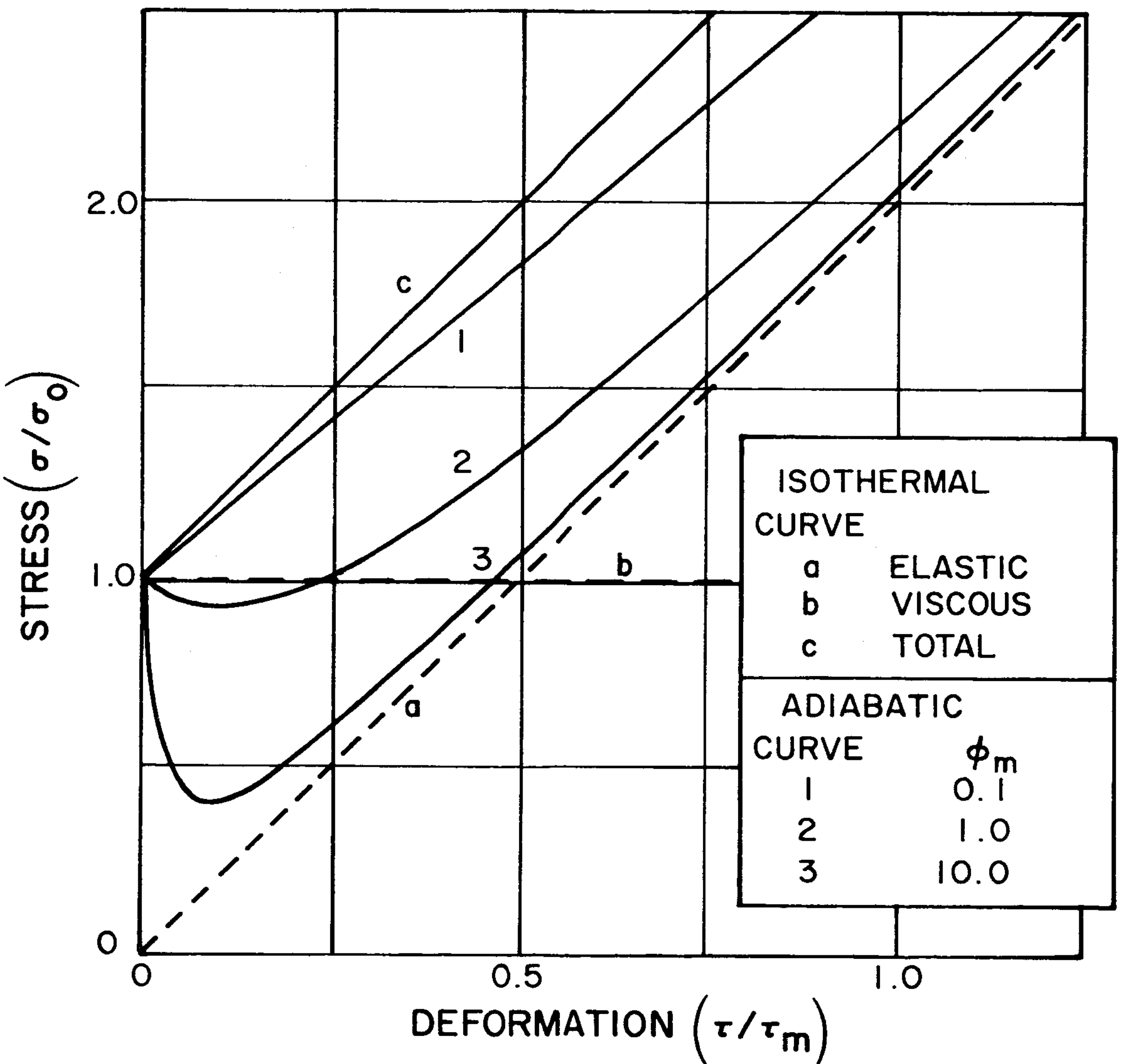

FIG. 8

N65 10679

Combined Thermal and Geometric Effects in Viscous Materials

By
I. J. Gruntfest
Re-Entry Systems Department
General Electric Co.
P. O. Box 8555
Philadelphia, Pa. 19101

July, 1964

ABSTRACT

10679

As part of a general study of the behavior of materials with temperature dependent properties, combined thermal and geometric effects in ideal viscous materials are explored analytically. The responses of cylinders to constant axial loads and to constant rates of axial deformation are computed. This continuum analysis is independent of, but complementary to, the contemporary solid state physics approach to the problem of the mechanical behavior of solids. The temperature coefficient of viscosity can be related to the atomic scale theory through the concept of the energy of activation for the flow process.

Non linear feedback effects occur both as a result of heating, and of shape change. In the tensile case these are both destabilizing. In the compressive case the geometric effects are stabilizing and the heating effects are destabilizing. One result of the analysis is therefore the prediction that the compressive deformation of a cylinder can occur rapidly at first, due to thermal feedback, and then be arrested due to geometric feedback. This is an effect familiar to students of metal forming processes.

Author

NOTATION

a - the temperature coefficient of viscosity of the working material.

A - the current cross section of the sample.

A_o - the initial cross section of the sample.

c - the temperature independent volumetric heat capacity of the material.

L - the current length of the sample.

L_o - the initial length of the sample.

$\mathcal{L}$ - the reduced length of the sample.

$\mathcal{L}_a$ - the reduced length in the adiabatic case.

$\mathcal{L}_i$ - the reduced length in the isothermal case.

P - the current load on the sample (σA).

P_o - the initial load on the sample.

P_a - the load in the adiabatic case.

P_i - the load in the isothermal case.

r - the rate of increase of $\mathcal{L}$ in the constant rate of deformation case.

t - the current time.

t_∞ - a convenient group of parameters having the dimensions of time. It is the time that would be required for the length to double in the adiabatic, no-shape change case.

t'_∞ - a convenient group of parameters having the dimensions of time. It is the time that would be required for the temperature to become unbounded in the adiabatic, no shape change case.

T - the current local temperature

T_o - the initial or reference temperature

α - a convenient group of parameters, the value of which indicates the relative importance of the thermal effects in the constant rate of deformation cases.

α' - a convenient group of parameters, the value of which indicates the relative importance of the thermal effects in the constant load cases.

β - the initial strain rate in the constant load case.

η - the temperature dependent, current, local viscosity.

η_0 - the viscosity at the reference temperature.

σ - the current value of the stress.

ϕ - the reduced temperature.

COMBINED THERMAL AND GEOMETRIC EFFECTS IN VISCOUS MATERIALS

INTRODUCTION

The flow and deformation of materials is a process which is at once exothermic and temperature sensitive. Under these conditions regenerative feedback (a chain reaction effect) is possible which can enhance the thermal effects and lead to instability. Some consequences of thermal feedback in selected, highly idealized model mechanical experiments have been discussed in earlier reports (1, 2). It was shown that thermal feedback could lead to yield and fracture in solids and to turbulence and cavitation in liquids.

Feedback effects and instability in mechanical experiments can also arise from purely geometric considerations. For example, when a constant tensile load is applied to a sample of material, the elongation is accompanied by a reduction in cross section so that the stress tends to increase producing positive feedback. Conversely, under a constant compressive load the stress tends to decrease so that the feedback is negative or degenerative.

In the present report, combined geometric and thermal effects are explored. The study of the combined effect is one of the many elaborations of the simple theory of thermal feedback in mechanical processes which might be undertaken. It turns out to be of some special interest because under selected conditions the feedback processes oppose one another. Experiments and processes in which this occurs may be particularly suitable for applying and testing the theory.

The model that is used in the analysis below is a cylinder of homogeneous, isotropic, incompressible viscous material subjected to a constant axial load or a constant axial elongation rate. The static adiabatic and isothermal behavior of this model are contrasted. The use of this model or of any homogeneous, isotropic continuum model ignores a great deal that is known about the physics of solids. However, it will be seen that this treatment is altogether complementary to the elegant and compelling atomic scale descriptions of the deformation of solids. One connection between the continuum and atomic scale theories is made through the temperature coefficient of the viscosity which is related to the energy of activation for the flow process. Another is through the appreciation of the temperature field in which the atomic scale events associated with the deformations occur.

The omission of elasticity, which can perhaps be remedied in the manner suggested in reference 2; is somewhat extravagant. On the other hand, geometric effects are not influential except for large deformations in which reversible or elastic effects are often not very significant.

The omission of heat conduction keeps the temperature and stress fields uniform. With heat conduction the interior of the cylinder would be hotter than the surface which might contribute to size effects and special surface effects which have often been noted in experiments.

Of the results given here, perhaps the most interesting relates to the compression of the model cylinder. There the stabilizing effect of the increase in cross section must overtake the destabilizing effect of the heating at some fraction of the original length of the cylinder. This may be related to what actually happens in certain forming operations applied to metals.

DISCUSSION OF THE ANALYSIS

In the earlier work (1), (2), geometric effects were avoided by discussing only the plane shear deformation of an infinite slab. The axial deformation of a cylinder which involves shape changes and which is considered in this report is also a viscometric experiment (3). The shear viscosity η is related to the axial load P by the equation

$$\frac{P}{A} = \sigma = \frac{3\eta}{\mathcal{L}} \frac{d\mathcal{L}}{dt} \tag{1}$$

in which A is the current uniform cross section of the cylinder, the factor 3 converts the shear viscosity to the tensile viscosity, σ is the current stress, t is time and $\mathcal{L}$ is the current reduced length which is defined in terms of the current length, L , and the initial length, L_o, by

$$\mathcal{L} = \frac{L}{L_o} = \frac{A_o}{A} \tag{2}$$

in which the incompressibility condition is applied.

CONSTANT RATE OF DEFORMATION

If in an isothermal experiment ($\eta = \eta_o$) the rate of change of length is a constant, $\frac{d\mathcal{L}}{dt} = r$, the current value of the load, P_i, is given by

(3) $$P_i = \sigma A = \left(\frac{3\eta_o}{\mathcal{L}} r \right)\left(\frac{A_o}{\mathcal{L}} \right) = \frac{P_o}{(1+rt)^2}$$

In the compression experiment, r is negative and P_i is always greater than P_o.

If now the deformation is considered to be adiabatic and the viscosity depends on temperature (as in reference (1) according to

(4) $$\eta = \eta_o e^{-a(T-T_o)} = \eta_o e^{-\phi}$$

in which T is the current temperature, T_o is the initial temperature, a is the temperature coefficient of the viscosity and ϕ is a reduced temperature defined by equation 4, the current load has the value

(5) $$P_a = \frac{3\eta_o r A_o e^{-\phi}}{(1+rt)^2} = \frac{P_o e^{-\phi}}{(1+rt)^2}$$

The value of ϕ can be obtained from the energy balance equation, which equates the mechanical work done to the local stored thermal energy

(6) $$P_a \frac{dL}{dt} = c L_o A_o \frac{dT}{dt}$$

in which c is the volumetric heat capacity, or

(7) $$\frac{3a\eta_o r^2}{c(1+rt)^2} e^{-\phi} = \frac{d\phi}{dt}$$

in which the variables can be separated to give

(8) $$e^{\phi}\, d\phi = \frac{1}{t_\infty} \frac{dt}{(1+rt)^2}$$

in which

(9) $$t_\infty = \frac{c}{3a\eta_0 r^2}$$

whence by integration

(10) $$e^{\phi} = \frac{-1}{r t_\infty (1+rt)} + \text{constant}$$

but since $\phi = 0$ for $t = 0$

(11) $$e^{\phi} = \frac{1+(1+\alpha)rt}{1+rt}$$

in which $\alpha = \frac{1}{rt_\infty}$

Whence it follows that

(12) $$P_a = \frac{P_0}{1+rt} \frac{1}{1+(1+\alpha)rt}$$

gives the adiabatic load history at constant rate of elongation or compression.

The load-deformation (or time) curves for tension are plotted in figure 1 for various values of α. The isothermal case corresponds to $\alpha = 0$. The load-deformation curves for compression are plotted in figure 2. Temperature histories for the two cases are shown in figures 3 and 4. In figure 1 it is seen that thermal feedback accentuates the load reduction due to the geometric effect. When α is sufficiently high the feedback due to geometric effects becomes negligible and the problem is similar to that discussed in reference 1.

In figure 2 it is seen that the feedback effects oppose each other. When $\alpha > 2$, the effects of thermal feedback are at first decisive, producing an initial load reduction which could appear as a mechanical instability which is arrested when the deformation or cross-sectional area becomes sufficiently high. This is a phenomenon which is similar to that which occurs when nail heads are formed on a wire. This idealized computation is likely to lead to a thinner head than is actually observed because, when heat conduction is taken into account, the hammer and anvil become more effective heat sinks as the axial length becomes smaller.

CONSTANT LOAD

When the load on the viscous cylinder is held at the constant value P_o, the stress will depend on time. In the isothermal case the deformation rate is given by (cf equation 1)

$$(13) \qquad \frac{1}{\mathcal{L}_i}\frac{d\mathcal{L}_i}{dt} = \frac{\sigma}{3\eta_o} = \frac{\sigma_o}{3\eta_o}\mathcal{L}_i = \frac{P_o}{3A_o\eta_o}\mathcal{L}_i$$

in which a tensile load is counted positive. Whence

$$(14) \qquad \frac{d\mathcal{L}_i}{\mathcal{L}_i^2} = \beta\, dt$$

where $\beta = \dfrac{\sigma_o}{3\eta_o} = \dfrac{P_o}{3A_o\eta_o}$

thus

$$(15) \qquad 1 - \frac{1}{\mathcal{L}_i} = \beta t$$

since $\mathcal{L}_i = 1$ when $t = 0$

or

$$(16) \qquad \mathcal{L}_i = \frac{1}{1-\beta t} .$$

When the adiabatic case is considered

$$(17) \qquad \frac{1}{\mathcal{L}_a}\frac{d\mathcal{L}_a}{dt} = \frac{\sigma}{3\eta_o}e^{\phi} = \frac{\sigma_o\mathcal{L}_a}{3\eta_o}e^{\phi} = \beta\mathcal{L}_a e^{\phi}$$

and ϕ must be determined from the energy equation (equation 6) in the form

$$(18) \qquad P_o\frac{a\mathcal{L}_a^2\sigma_o L_o}{3\eta_o}e^{\phi} = c\, L_o A_o \frac{d\phi}{dt}$$

or

$$(19) \qquad e^{\phi} = \frac{3c\eta_0 A_0}{a P_0 \sigma_0} \frac{1}{\mathcal{L}_a^2} \frac{d\phi}{dt} = \frac{t'_\infty}{\mathcal{L}_a^2} \frac{d\phi}{dt}$$

in which $t'_\infty = \frac{3c\eta_0 A_0}{a P_0 \sigma_0} = \frac{3c\eta_0 A_0^2}{a P_0^2}$

Substituting 19 into 17

$$(20) \qquad \frac{1}{\mathcal{L}_a^2} \frac{d\mathcal{L}_a}{dt} = \beta \frac{t'_\infty}{\mathcal{L}_a^2} \frac{d\phi}{dt}$$

whence, integrating, we find a relationship between the length and temperature

$$(21) \qquad \phi = \frac{1}{\beta t'_\infty} (\mathcal{L}_a - 1) = \alpha' (\mathcal{L}_a - 1)$$

in which $\alpha' = \frac{1}{\beta t'_\infty}$

This can now be substituted into the energy equation (equation 19) to obtain a relationship between length and time which is the solution to the ideal adiabatic constant load problem. We have then

$$(22) \qquad e^{-\alpha'} e^{\alpha' \mathcal{L}_a} = \frac{t'_\infty}{\mathcal{L}_a^2} \frac{d(\alpha' \mathcal{L}_a)}{dt}$$

or separating variables and integrating

$$(23) \qquad \frac{e^{-\alpha'}}{\alpha' t'_\infty} t = \int_{\mathcal{L}_a = 1}^{\mathcal{L}_a} \frac{e^{-\alpha' \mathcal{L}_a}}{\mathcal{L}_a^2} d\mathcal{L}_a$$

The indicated integration in equation 23 can be performed by parts to give

$$(24) \qquad \frac{e^{-\alpha'}}{\alpha'^2} \frac{t}{t'_\infty} = - \left. \frac{e^{-\alpha' \mathcal{L}_a}}{\alpha' \mathcal{L}_a} \right|_{\mathcal{L}_a = 1}^{\mathcal{L}_a} - \int_{\alpha' \mathcal{L}_a = \alpha'}^{\alpha' \mathcal{L}_a} \frac{e^{-\alpha' \mathcal{L}_a}}{\alpha' \mathcal{L}_a} d(\alpha' \mathcal{L}_a)$$

which is computed from tabulated functions for various values of $\alpha' \mathcal{L}_a$ to get the relationship between $\mathcal{L}_a$ and t.

For the preparation of Table I we let

$$(25) \qquad f(\alpha\mathcal{L}) = \frac{e^{-\alpha\mathcal{L}}}{\alpha\mathcal{L}} + \int_{-\infty}^{\alpha\mathcal{L}} \frac{e^{-\alpha\mathcal{L}}}{\alpha\mathcal{L}} \, d(\alpha\mathcal{L})$$

so that

$$(26) \qquad \frac{e^{-\alpha'}}{\alpha'^2} \frac{t}{t'_\infty} = f(\alpha') - f(\alpha'\mathcal{L}_a)$$

It can be shown that for large values of $\alpha'\mathcal{L}_a$

$$(27) \qquad \frac{e^{-\alpha'}}{\alpha'^2} \frac{t}{t'_\infty} \doteq \frac{e^{-\alpha'}}{\alpha'^2} - \frac{e^{-\alpha'\mathcal{L}_a}}{(\alpha'\mathcal{L}_a)^2}$$

and for small $\alpha'\mathcal{L}_a$

$$(28) \qquad \frac{e^{-\alpha'}}{\alpha'^2} \frac{t}{t'_\infty} \doteq \frac{1}{\alpha'} - \frac{1}{\alpha'\mathcal{L}_a}$$

For intermediate values of $\alpha'\mathcal{L}_a$ Table I is used.

The results of the computations using equation 26 are shown in figures 5 and 6 for constant tensile and constant compressive load respectively. Here again the dramatic stabilization of the compressed material at some fraction of its original length is shown along with the enhancement of the tensile instability by the combined geometric and thermal effects. The corresponding temperature histories (equation 21) are linear and need not be plotted.

CONCLUDING DISCUSSION AND ACKNOWLEDGEMENTS

The study presented above is part of a continuing program of study of the behavior of materials with temperature dependent properties. While the model is highly idealized, the analysis further strengthens the view that the application of the first law of thermodynamics may be useful for understanding the mechanical behavior of real materials.

Two points are made. First, it is shown to be possible to rationalize, qualitatively, a technologically important type of deformation of solids. Second, a possible way of bridging the gap between the equally elegant but isolated continuum and atomistic theories of solid behavior is suggested.

This work was made possible by the encouragement and support of the Office of Advanced Research and Technology of the National Aeronautics and Space Administration under Contract NASw 708 monitored by Messrs. Howard Wolko and Melvin Rosche'. The author is indebted to his colleague, Mr. George Mueller, for helpful discussions and assistance in performing the computations.

Bibliography

1. Gruntfest, I. J. "Apparent Departures from Newtonian Behavior in Liquids Caused by Viscous Heating", Pro-Proposed for 35th Annual Meeting of the Society of Pheology, Pittsburgh, Pa. October 1964.

2. Gruntfest, I. J., and S. J. Becker, "Thermal Effects in Model Visco-Elastic Solids", Proposed for 6th Annual Structures and Materials Conference AIAA, Palm Springs Cal. April 1965.

3. Fox, T. G., Gratch, S., and Loshaek, S., "Visometric Techniques" in book "Rheology", edited by F. Eirich, Academic Press New York (1956)(Vol. I page 434)

CAPTIONS FOR FIGURES

#1 The tensile load (P_a/P_o) versus the elongation ($\mathcal{L}-1$) in the adiabatic constant rate of elongation case for various values of α.

#2 The compressive load (P_a/P_o) versus the compression ($1-\mathcal{L}$) in the adiabatic constant rate of compression case for various values of α.

#3 The reduced temperature (ϕ_a) versus the elongation ($\mathcal{L}-1$) in the adiabatic constant rate of elongation case for various values of α.

#4 The reduced temperature (ϕ_a) versus the compression ($1-\mathcal{L}$) in the adiabatic constant rate of compression case for various values of α.

#5 The reduced length ($\mathcal{L}$) versus time (βt) at constant tensile load under adiabatic conditions for various values of α.

#6 The reduced length ($\mathcal{L}$) versus time (βt) at constant compressive load under adiabatic conditions for various values of α.

TABLE I

$\frac{e^{\alpha}}{\alpha}$ AND $f(\alpha)$ FOR INTERMEDIATE VALUES OF α
(for finding $\mathcal{L}_a(t)$ with equation 26)

α	$\frac{e^{-\alpha}}{\alpha}$	$f(\alpha)$ Tension	$-\frac{e^{\alpha}}{\alpha}$	$f(-\alpha)$ Compression
.01	99.005	94.967	101.01	-105.02
.02	49.009	45.655	51.01	- 54.32
.03	32.346	29.387	34.35	- 37.22
.04	24.019	21.328	26.02	- 28.63
.05	19.024	16.556	21.03	- 23.39
.06	15.696	13.401	17.69	- 19.86
.07	13.319	11.169	15.32	- 17.33
.08	11.579	9.553	13.54	- 15.41
.09	10.154	8.236	12.16	- 13.90
.10	9.048	7.225	11.05	- 12.67
.2	4.094	2.8709	6.107	- 6.929
.3	2.469	1.5636	4.500	- 4.802
.4	1.676	.9734	3.729	- 3.834
.5	1.213	.6533	3.297	- 2.843
.6	.9147	.4603	3.037	- 2.267
.7	.7094	.3356	2.868	- 1.803
.8	.5617	.2511	2.782	- 1.445
.9	.4517	.1915	2.733	- 1.111
1.0	.3679	.1484	2.718	- .823
1.1	.3026	.11662	2.731	- .5637
1.2	.2510	.09257	2.767	- .3246
1.3	.2096	.07419	2.823	- .1011
1.4	.1757	.05948	2.897	.1106
1.5	.1487	.04873	2.988	.3135
1.6	.1256	.03925	3.096	.5097
1.7	.1075	.03281	3.220	.7011
1.8	.0918	.02712	3.361	.8890
1.9	.0787	.02249	3.524	1.069
2.	.06767	.01876	3.695	1.260
3.	.01659	.003547	6.695	3.238
4.	.004579	.000800	13.649	5.981
5.	.001349	.000201	29.68	10.50
6.	.0004131	.0000520	67.24	18.74
7.	.0001303	.0000147	156.66	34.84
8.	.00004194	.00000427	372.63	67.75
9.	.00001349	.00000104	900.35	137.5
10.	.000004540	.000000383	2202.6	289.6
11.	.000001518	.00000012	5443.	628.4
12.	.00000051	.00000004	13562.	1397.

CONSTANT RATE OF ELONGATION

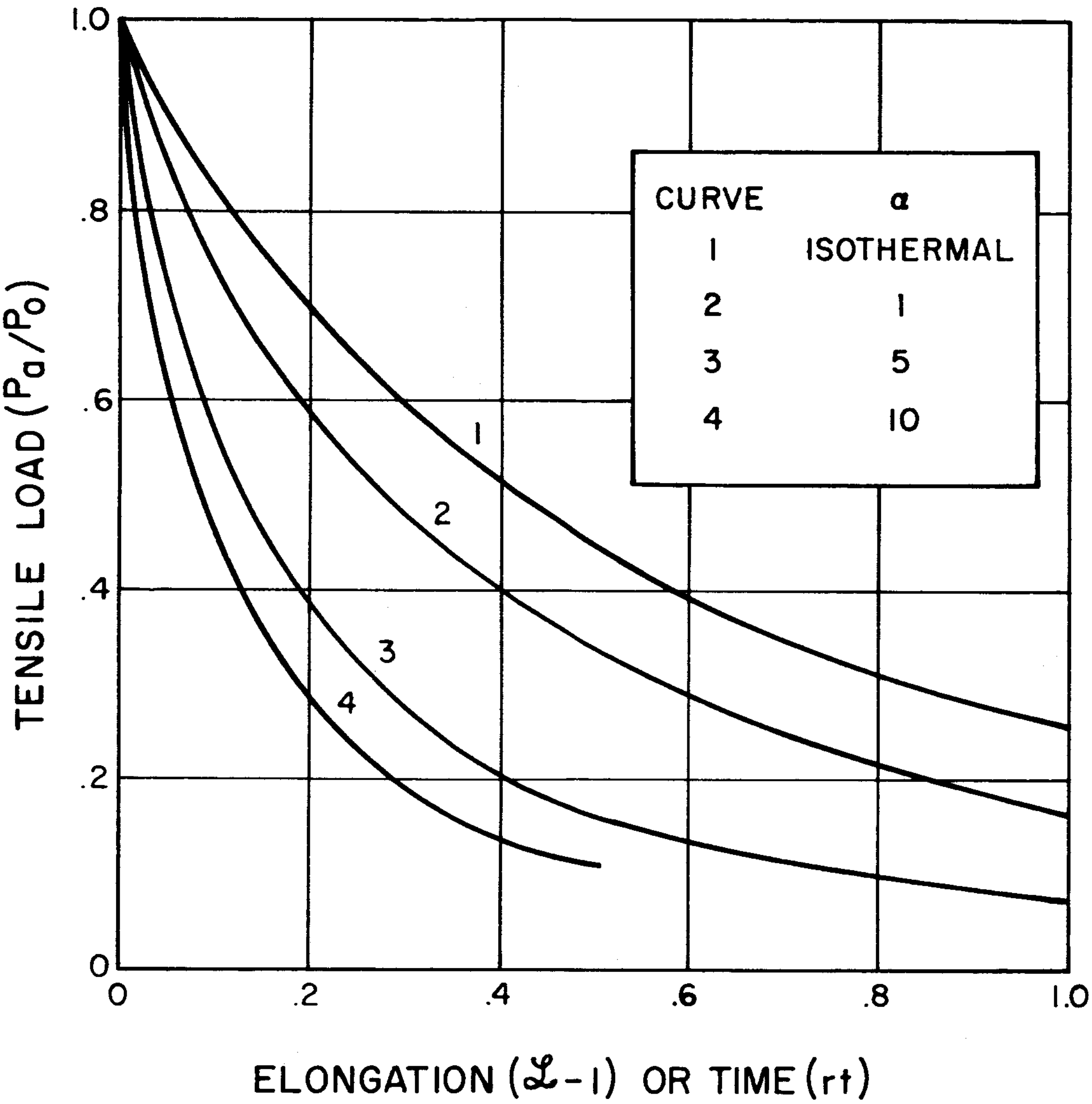

FIG. 1

CONSTANT RATE OF COMPRESSION

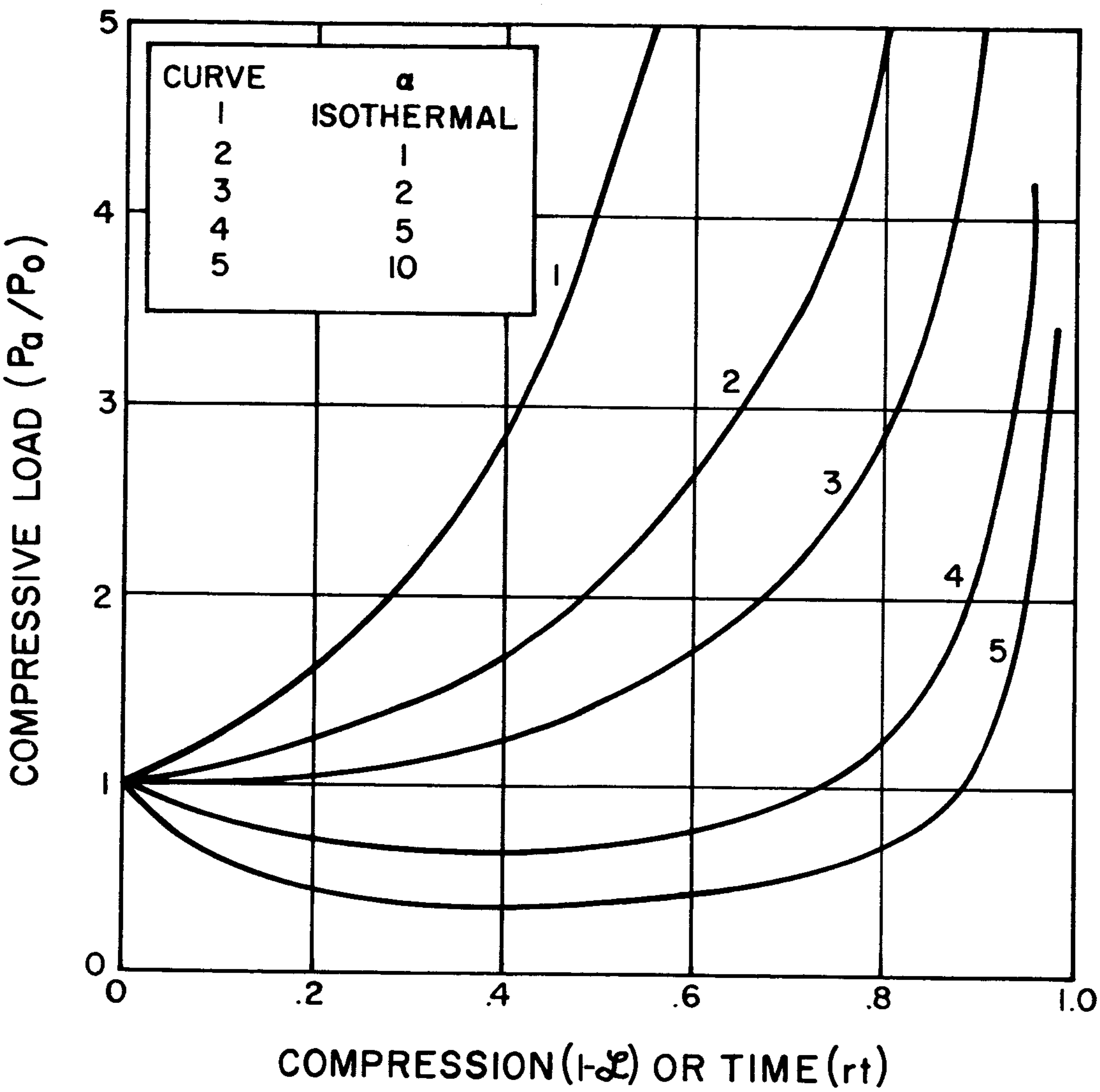

FIG. 2

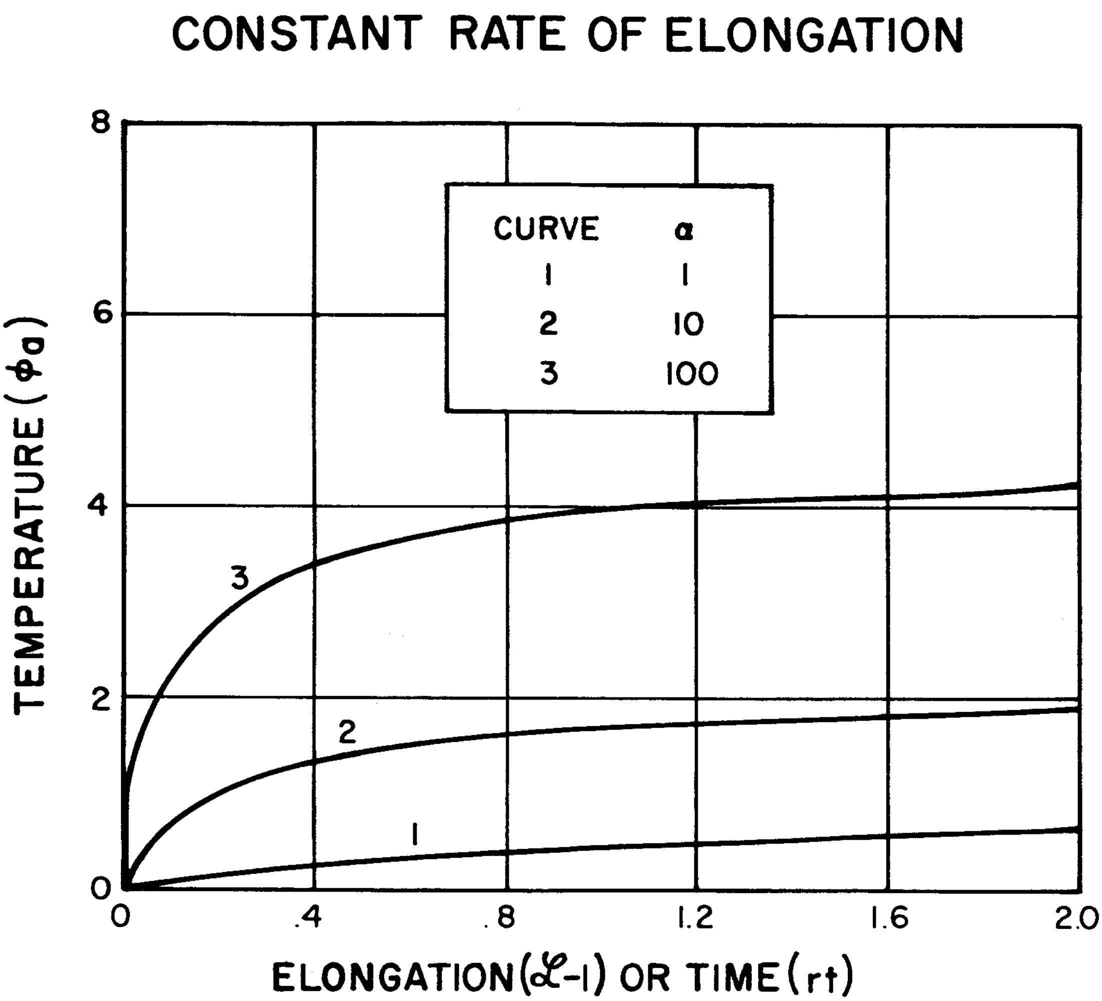

CONSTANT RATE OF ELONGATION
CURVE α
1 1
2 10
3 100
TEMPERATURE (φa)
ELONGATION(ℒ-1) OR TIME(rt)
0
.4
.8
1.2
1.6
2.0
2
4
6
8

FIG. 3

CONSTANT RATE OF COMPRESSION

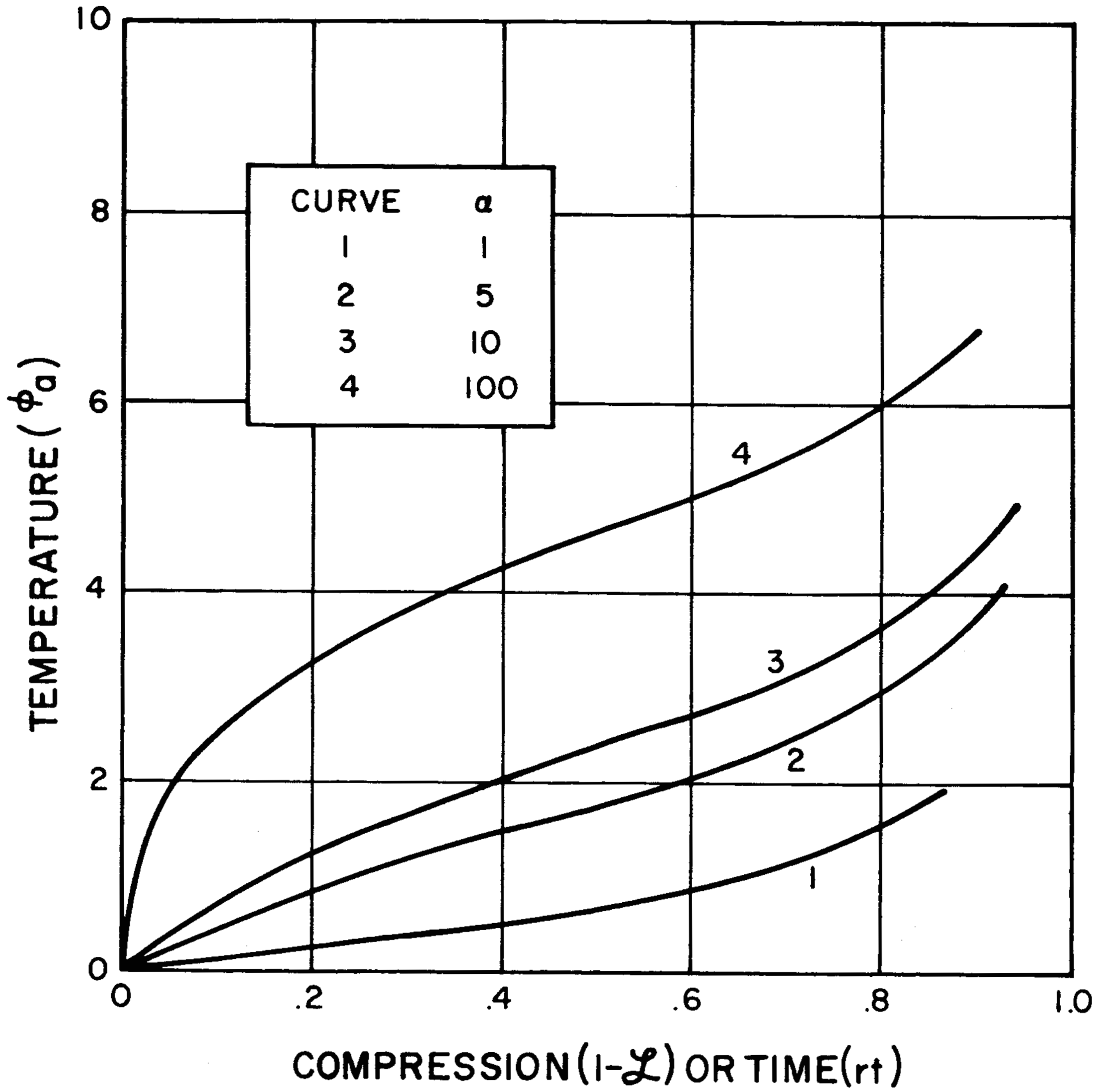

FIG. 4

CONSTANT LOAD

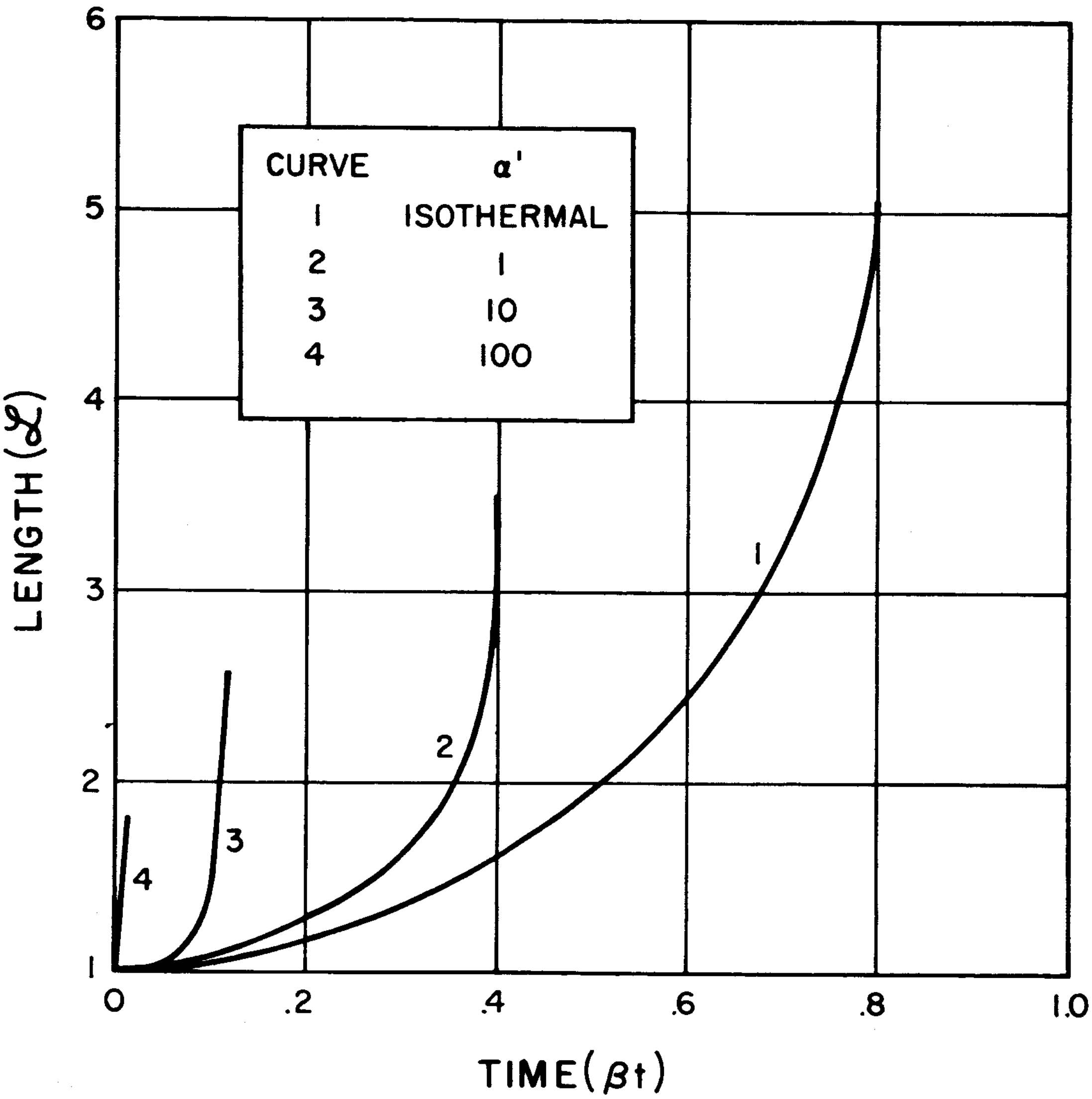

FIG. 5

CONSTANT LOAD

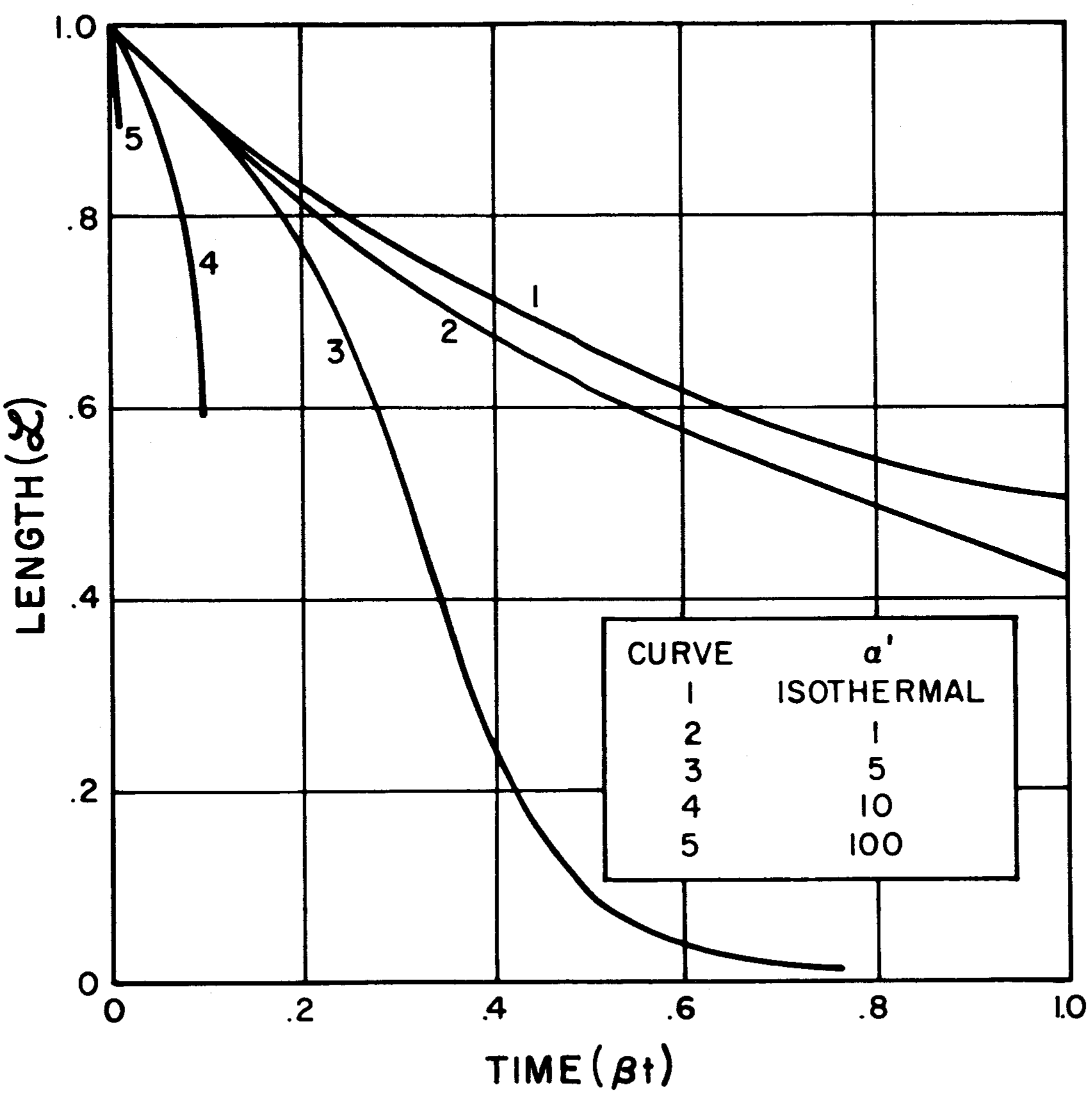

FIG. 6